

DESIGN AND SIMULATION OF A VAPOR COMPRESSION REFRIGERATION  
CYCLE FOR A MICRO REFRIGERATOR

A THESIS SUBMITTED TO  
THE GRADUATE SCHOOL OF NATURAL AND APPLIED SCIENCES  
OF  
MIDDLE EAST TECHNICAL UNIVERSITY

BY

SEYFETTİN YILDIZ

IN PARTIAL FULLFILLMENT OF THE REQUIREMENTS  
FOR  
THE DEGREE OF MASTER OF SCIENCE  
IN  
MECHANICAL ENGINEERING

JUNE 2010

Approval of the thesis:

**DESIGN AND SIMULATION OF A VAPOR COMPRESSION REFRIGERATION  
CYCLE FOR A MICRO REFRIGERATOR**

submitted by **SEYFETTİN YILDIZ** in partial fulfillment of the requirements for the degree  
of **Master of Science in Mechanical Engineering Department, Middle East Technical  
University** by,

Prof. Dr. Canan Özgen  
Dean, Graduate School of **Natural and Applied Sciences**

Prof. Dr. Suha Oral  
Head of Department, **Mechanical Engineering**

Asst. Prof. Dr. H. Tuba Okutucu Özyurt  
Supervisor, **Mechanical Engineering Dept., METU**

Prof. Dr. Rüknettin Oskay  
Co-Supervisor, **Mechanical Engineering Dept., METU**

**Examining Committee Members:**

Assist. Prof. Dr. İlker Tari  
Mechanical Engineering Dept., METU

Assist. Prof. Dr. H. Tuba Okutucu Özyurt  
Mechanical Engineering Dept., METU

Prof. Dr. Rüknettin Oskay  
Mechanical Engineering Dept., METU

Assist. Prof. Dr. Cüneyt Sert  
Mechanical Engineering Dept., METU

Assoc. Prof. Dr. Haluk Külâh  
Electrical and Electronics Engineering Dept., METU

**Date:**

**I hereby declare that all information in this document has been obtained and presented in accordance with academic rules and ethical conduct. I also declare that, as required by these rules and conduct, I have fully cited and referenced all material and results that are not original to this work.**

Name, Last name : Seyfettin YILDIZ

Signature :

## **ABSTRACT**

### **DESIGN AND SIMULATION OF A VAPOR COMPRESSION REFRIGERATION CYCLE FOR A MICRO REFRIGERATOR**

YILDIZ, Seyfettin

M.S., Department of Mechanical Engineering

Supervisor: Asst. Prof. Dr. Tuba OKUTUCU ÖZYURT

Co-Supervisor: Prof. Dr. Rüknettin OSKAY

June 2010, 108 pages

Cooling of electronic equipments has become an important issue as the advances in technology enabled the fabrication of very small devices. The main challenge in cooling is the space limitation. The use of miniature refrigerators seems to be a solution alternative for the cooling problem.

The objective of this study is to design and simulate a vapor compression refrigeration cycle for a micro-scale refrigerator. A MATLAB code is developed for the simulations. The four components of the refrigerator, namely, the condenser, evaporator, compressor and the capillary tube are designed separately. The cycle is successfully completed nearly at the same point where it begins.

The cold space temperature, ambient air temperature, condensation and evaporation temperatures, and the evaporator heat load are the predetermined parameters. A fan

is used to cool the condenser, and the compressor is selected as isentropic.

R-134A is selected as the refrigerant and a simple interpolation code is developed to obtain the thermophysical properties of R-134A.

The original design is carried out with an isentropic compressor. For the purpose of comparison, a cycle with a polytropic compressor is also considered. Similarly, two alternative designs for the evaporator are developed and simulated. A second law analysis is performed at the end of the study.

Keywords: Micro refrigerator, electronic cooling, micro evaporator-condenser, microchannels, vapor compression refrigeration cycle.

## ÖZ

### **BİR MİKRO BUZDOLABI İÇİN BUHAR SIKIŞTIRMALI SOĞUTMA DÖNGÜSÜNÜN TASARIMI VE BENZETİMİ**

YILDIZ, Seyfettin

Yüksek Lisans, Makina Mühendisliği Bölümü

Tez Yöneticisi: Y. Doç. Dr. Tuba OKUTUCU ÖZYURT

Ortak Tez Yöneticisi: Prof. Dr. Rüknettin OSKAY

Haziran 2010, 108 sayfa

Günümüzde, üretim teknolojilerindeki gelişmeler sayesinde elektronik cihaz boyutlarının giderek küçülmesi soğutma problemini de beraberinde getirmiştir. Elektronik soğutma konusundaki temel zorluk alan sıkışıklıdır. Minyatür soğutucuların kullanımı, soğutma problemine bir çözüm alternatifi olarak görünmektedir.

Bu çalışmanın amacı mikro ölçekli, buhar sıkıştırırmalı bir soğutma döngüsünün tasarımını ve bilgisayar ortamında benzetimini gerçekleştirmektir. Bu maksatla bir MATLAB kodu geliştirilmiştir. Soğutma döngüsünün dört ana bileşeni olan kondenser, evaporator, kompresör ve kılcal boru ayrı ayrı tasarlanmıştır. Döngünün başladığı noktayla neredeyse aynı noktada bitmesi sağlanmıştır.

Soğuk oda sıcaklığı, ortam sıcaklığı, yoğuşma ve buharlaşma sıcaklıkları ile soğutma yükü önceden belirlenen parametrelerdir. Kondenseri soğutmak amacıyla bir fan kullanılmış; adiyabatik, izentropik bir kompresör seçilmiştir.

Soğutucu akışkan olarak R-134A seçilmiş ve termodinamik özellikleri okumak için basit bir interpolasyon kodu yazılmıştır.

İlk tasarım, sabit entropili bir kompresör ile yapılmıştır. Karşılaştırma amaçlı olarak, politropik kompresörlü bir döngü de incelenmiştir. Benzer şekilde, evaporator için de iki farklı tasarım geliştirilmiş ve benzetimleri yapılmıştır. Çalışmanın sonunda ikinci yasa analizi de gerçekleştirilmiştir.

Anahtar Kelimeler: Mikro buzdolabı, elektronik soğutma, mikro buharlaştırıcı-yoğuşturucu, mikrokanallar, buhar sıkıştırımlı soğutma döngüsü.

## **ACKNOWLEDGEMENTS**

I would like to express my sincere thanks to Dr. Rüknettin OSKAY and Dr. Tuba OKUTUCU ÖZYURT for their perfect guidance, support and endless patience during this long period of thesis study.

I would like to thank to my colleague Dr. M. Umut Halilođlu for his supports in this period.

In addition, a thank to all of my friends who were always near me.

Very special thanks to my father, mother and Zuhall who share the life with me.

## TABLE OF CONTENTS

ABSTRACT.....	iv
ÖZ.....	vi
ACKNOWLEDGEMENTS .....	viii
LIST OF SYMBOLS AND ABBREVIATIONS .....	xiv
CHAPTERS	
1. INTRODUCTION .....	1
1.1 General .....	1
1.2 Traditional Vapor Compression Refrigeration Cycle .....	2
1.3 Micro-Scale Vapor Compression Refrigeration Cycle .....	4
1.3.1 What is meant by micro?.....	4
1.3.2 History of Micro VCRC.....	6
1.3.2.1 Literature on Evaporation in Microchannels .....	7
1.3.2.2 Literature on Condensation in Microchannels .....	8
1.3.2.3 Literature on Micro VCRC .....	9
1.4 The Objective of the Study .....	11
2. EVAPORATOR DESIGN .....	13
2.1 Geometry and Material Selection.....	13
2.2 Operational Conditions .....	15
2.3 Heat Transfer and Pressure Drop Calculations .....	15
2.3.1 Two Phase Flow .....	16
2.3.2 Single Phase Flow .....	21
2.3.3 Fin Analysis .....	22
2.4 Alternative Evaporator Design.....	23
3. COMPRESSOR DESIGN.....	25
3.1 General .....	25

3.2 Principle Dimensions and Working Principles .....	25
3.3 Compressor Work .....	28
3.4 Compressor Performance .....	29
3.5 Compressor Speed.....	30
4. CONDENSER DESIGN .....	31
4.1 Geometry and Material .....	31
4.2 Operational Conditions .....	35
4.3 Calculation Scheme.....	35
4.4 Refrigerant Side Heat Transfer and Pressure Drop Calculations.....	36
4.4.1 Single Phase Flow .....	36
4.4.2 Two Phase Flow .....	38
4.5 Air-Side Heat Transfer and Pressure Drop Calculations .....	41
4.6 Overall Heat Transfer Calculations.....	43
5. CAPILLARY TUBE DESIGN .....	45
5.1 Introduction .....	45
5.2 Sizing of the Capillary Tube .....	46
5.3 Pressure Drop in the Capillary Tube.....	46
6. SECOND LAW ANALYSIS .....	52
6.1 General Considerations .....	52
7. SIMULATIONS.....	54
7.1 General .....	54
7.2 Algorithm .....	54
7.3 Design and Simulation of a Micro VCRC .....	56
7.3.1 Evaporator .....	56
7.3.1.1 Two Phase Mixture Regime .....	57
7.3.1.2 Single Phase Regime .....	60
7.3.2 Compressor Design .....	62
7.3.3 Condenser Design .....	63
7.3.3.1 Superheated Vapor Regime.....	64
7.3.3.2 Two Phase Mixture Condensation Regime.....	66
7.3.4 Capillary Tube.....	70
8. RESULTS. ....	72

8.1 General .....	72
8.2 Results of Micro VCRC with Isentropic Compressor.....	72
8.3 Results of Micro VCRC with Polytropic Compressor .....	79
9. DISCUSSION AND CONCLUSION.....	84
9.1 Discussion and Conclusion .....	84
9.2 Future Work .....	88
REFERENCES.....	90
APPENDICES	
A. PRESSURE VS. ENTHALPY CURVE OF R-134A .....	96
B. SATURATED LIQUID AND VAPOR PROPERTIES OF R-134A.....	97
C. SAMPLE CALCULATIONS.....	98
C.1 Evaporator Part.....	98
C.1.1 Two-Phase Region.....	98
C.1.2 Single-Phase Region.....	100
C.2 Compressor Part .....	101
C.3 Condenser Part .....	101
C.3.1 Single-Phase Region.....	102
C.3.2 Two-Phase Region.....	103
C.4 Capillary Tube Part.....	107

## LIST OF FIGURES

Figure 1. 1 Refrigeration Process .....	2
Figure 1. 2 Basic Components of a Sample VCRC .....	2
Figure 1. 3 Temperature vs. Entropy Diagram of an Ideal VCRC .....	3
Figure 1. 4 Pressure vs. Enthalpy Diagram of an Ideal VCRC.....	3
Figure 2. 1 Isometric View of the Evaporator.....	13
Figure 2. 2 Evaporator Assembly .....	14
Figure 2. 3 Alternative Evaporator.....	24
Figure 3. 1 Basic Geometry of Compressor.....	26
Figure 3. 2 Pressure vs. Volume Diagram .....	26
Figure 3. 3 Suction and Discharge Pressures .....	28
Figure 4. 1 Condenser Geometry .....	31
Figure 4. 2 Fin Geometry .....	32
Figure 4. 3 Principle Dimensions of Condenser .....	33
Figure 5. 1 Capillary Tube Section .....	46
Figure 5. 2 Segmentation in capillary tube .....	50
Figure 5. 3 Choked Flow Condition.....	51
Figure 7. 1 Design Algorithm .....	55
Figure 8. 1 Condensation Heat Transfer Coefficient ( $W/m^2K$ ) vs. Length (mm).....	76
Figure 8. 2 Heat Transfer Coefficients ( $W/m^2K$ ) vs. Length (mm).....	76
Figure 8. 3 Reynolds Number vs. Length (mm) .....	77
Figure 8. 4 Temperature vs. Entropy with Isentropic Compressor .....	78
Figure 8. 5 Pressure vs. Enthalpy with Isentropic Compressor .....	79
Figure 8. 6 Temperature vs. Entropy with Polytropic Compressor .....	82
Figure 8. 7 Pressure vs. Enthalpy with Polytropic Compressor.....	83
Figure A. 1 Pressure vs. Enthalpy Curve of R-134A.....	96

## LIST OF TABLES

Table 1. 1 Flow Regimes for Different Gases.....	5
Table 1. 2 Channel Classifications.....	5
Table 2. 1 Principle Dimensions of the Evaporator .....	14
Table 2. 2 Operational Conditions of the Evaporator .....	15
Table 2. 3 Nusselt Number Values for Rectangular Ducts [29] .....	20
Table 4. 1 Principle Dimensions .....	32
Table 4. 2 Design Variables of the Condenser.....	35
Table 8. 1 Evaporator Results .....	73
Table 8. 2 Alternative Evaporator Results .....	73
Table 8. 3 Compressor Results .....	74
Table 8. 4 Condenser Results.....	75
Table 8. 5 Capillary Tube Design .....	77
Table 8. 6 Cycle Parameters .....	78
Table 8. 7 Evaporator Results .....	79
Table 8. 8 Alternative Evaporator Results .....	80
Table 8. 9 Compressor Results .....	80
Table 8. 10 Condenser Results.....	81
Table 8. 11 Capillary Tube Design .....	81
Table 8. 12 Cycle Parameters.....	82
Table 9. 1 Comparison of present study with literature .....	88
Table B. 1 Saturation Properties of R-134A .....	97
Table C. 1 Refrigerant Side Results.....	106
Table C. 2 Air Side Results.....	107
Table C. 3 Capillary Tube Results .....	108

## LIST OF SYMBOLS AND ABBREVIATIONS

$A$	Area
BDC	Bottom dead center
$Bo$	Boiling number
$Co$	Confinement number, convection number
$COP$	Coefficient of performance
$D$	Diameter
$f$	Friction coefficient
$F$	Correction factor, force
$S$	Fluid surface parameter
$G$	Mass flux
$H$	Channel height
$g$	Gravitational acceleration
$h$	Convective heat transfer coefficient
$I$	Irreversibility
$i$	Enthalpy
$j$	Super-facial velocity
$k$	Thermal conductivity
$k$	Isentropic index
$l$	Louver
$L$	Laplace constant, length
$\dot{m}$	Mass flow rate
$M$	Momentum
$N$	Number of channels, rotational speed
$Nu$	Nusselt value
$P$	Pressure, wetted perimeter
$Po$	Poiseuille number

$Pr$	Prandtl number
$q''$	Heat flux
$Re$	Reynolds number
$s$	Entropy
$S$	Fluid surface parameter
$T$	Temperature
$t$	Thickness
TDC	Top dead center
$U$	Velocity
$u$	Dimensionless velocity
$V$	Volume, velocity
$W$	Work
$w$	Channel width, specific work
$We$	Weber number
$x$	Vapor fraction
$z$	Fin

Greek Letters:

$X$	Martinelli parameter
$\Delta$	Difference
$\delta$	Film thickness
$\varepsilon$	Effectiveness
$\eta$	Efficiency
$\phi$	Two phase multiplier
$\varphi$	Surface tension parameter
$\mu$	Dynamics viscosity
$\nu$	Specific density
$\theta$	Louver angle
$\rho$	Density

$\sigma$	Surface tension
$\tau$	Shear stress

Subscripts:

a	Air
acc	Accelerational
b	Base
c	Corrected, clearance
ch	Channel
cl	Clearance
CB	Convective boiling
CR	Cold room
cu	Copper
CV	Control volume
d	Depth
f	Frictional
GN	Gnielinski
h	Hydraulic
i	Interfacial, inner side
init	Initial
l	Liquid phase, length
lo	Liquid only
lv	Liquid to vapor
m	Mean
NB	Nucleate boiling
o	Overall, outer side
p	Pitch, swept
pd	Discharge pressure fraction
ps	Suction pressure fraction

r	Refrigerant
s	Suction
seg	Segment
sp	Single phase
st	Stroke
t	Tube side, thickness
tp	Two phase
v	Vapor phase
vol	Volumetric

## CHAPTER 1

### INTRODUCTION

#### 1.1 General

Since Jacob Perkin's "Ice Machine" built in 1834, Vapor Compression Refrigeration Cycle (VCRC) has been in service of human beings. It can be used whenever a refrigeration or air-conditioning requirement occurs. For a decade, due to the tendency of miniaturization in technology, an effort to produce this refrigeration cycle in smaller scales has begun, as well. Some application areas of micro refrigerators may be sorted as:

- Space and aviation industry
- Military purposes
- Automotive industry
- Biomedical studies
- Micro electro mechanical systems (MEMS)

Especially, in hot spot applications, micro refrigerators take an important role due to their advantages, such as the compactness, high COP values, ultra-low cold plate temperatures and low mass flow rates.

## 1.2 Traditional Vapor Compression Refrigeration Cycle

The common VCRC has four main components that are the condenser, expansion valve, evaporator and the compressor. The major function of a refrigerator is to create a cold region by rejecting heat to the ambient as illustrated in Figure 1.1.

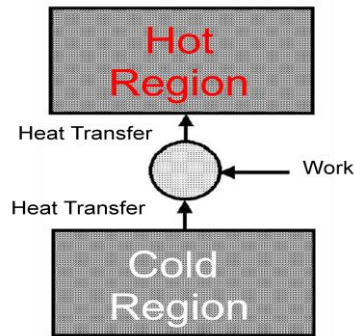


**Figure 1. 1** Refrigeration Process

The basic components of a sample VCRC are given in Figure 1.2 below.

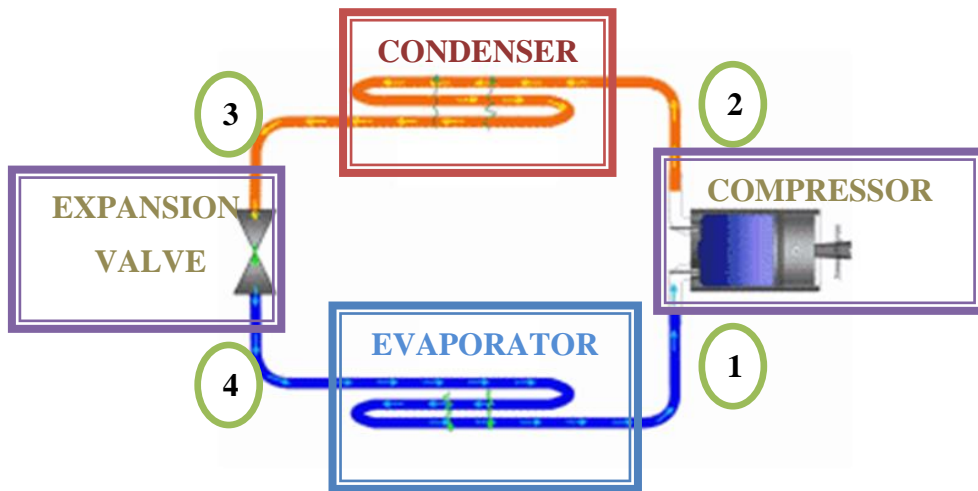


**Figure 1. 2** Basic Components of a Sample VCRC

The pressure vs. enthalpy and temperature vs. entropy diagrams of an ideal VCRC are given in Figures 1.3 and 1.4., respectively.

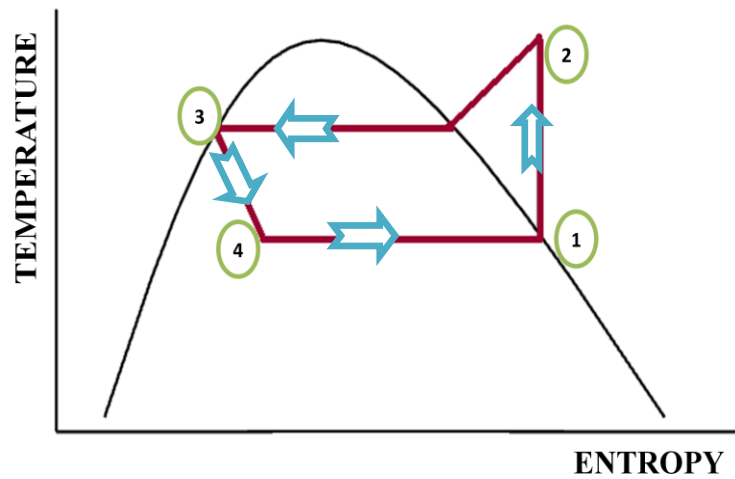


**Figure 1. 3** Temperature vs. Entropy Diagram of an Ideal VCRC

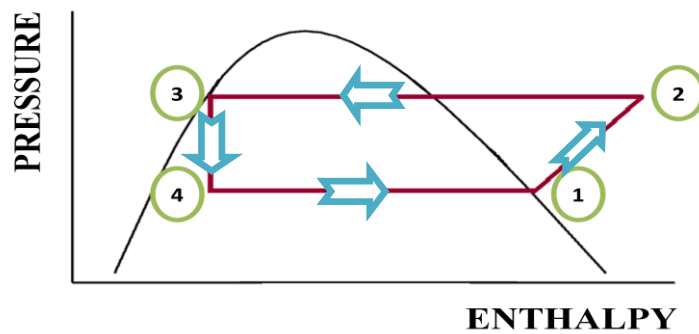


**Figure 1. 4** Pressure vs. Enthalpy Diagram of an Ideal VCRC

Referring to Figures 1.2-4, the functions of the four main components of an ideal VCRC may be summarized as follows:

**1-2 Compressor:** The low pressure saturated vapor is compressed to a high pressure superheated vapor under constant entropy value.

**2-3 Condenser:** The high pressure superheated vapor is sub-cooled to a saturated vapor state and then condenses into a saturated liquid state under constant pressure.

**3-4 Expansion Valve:** The high-pressure saturated liquid is expanded to a low pressure and temperature liquid-vapor mixture at constant enthalpy.

**4-1 Evaporator:** The low-pressure two-phase mixture boils to saturated vapor under constant pressure.

It is a fact that the ideal cycle can nearly never be realized, especially in micro-channel VCRCs owing to the very small dimensions of the channels, and much higher pressure drops. Hence, in this study, the pressure drops in the condenser and the evaporator have been taken into account. On the other hand, a miniature isentropic compressor has been selected.

### 1.3 Micro-Scale Vapor Compression Refrigeration Cycle

#### 1.3.1 What is meant by micro?

The categorization of channels according to their sizes is not an easy task due to various dissimilar views in the community. As reported in the study of Mehendale, Jacobi and Shah [1], channels are classified into four types according to their hydraulic diameters:

- $1 \mu\text{m} < D_h < 100 \mu\text{m}$  : Microchannels
- $100 \mu\text{m} < D_h < 1 \text{mm}$  : Meso-channels
- $1 \text{mm} < D_h < 6 \text{mm}$  : Compact passages
- $D_h > 6 \text{mm}$  : Conventional channels

In addition to these, Kandlikar et. al. [2] elaborate on the micro-channel flow and thermo-hydraulic performance, pointing out the flow regime effect of different gases. The flow regimes are classified as shown in Table 1.1 under 1 atmosphere pressure.

**Table 1. 1** Flow Regimes for Different Gases

Channel Dimensions ( $\mu\text{m}$ )				
Gas	Continuum Flow	Slip Flow	Transition Flow	Free Molecular Flow
<b>Air</b>	> 67	0.67- 67	0.0067-0.67	< 0.0067
<b>Helium</b>	> 194	1.94-194	0.0194-1.94	< 0.0194
<b>Hydrogen</b>	> 123	1.23-123	0.0123-1.23	< 0.0123

In the same study of Kandlikar et al. [2], channel classification based on the hydraulic diameter is given as shown in Table 1.2.

**Table 1. 2** Channel Classifications

Channel Class	Channel Hydraulic Diameter
Conventional Channel	> 3 mm
Mini-Channel	200 $\mu\text{m}$ to 3mm
Micro-Channel	10 $\mu\text{m}$ to 200 $\mu\text{m}$
Transitional Micro-Channel	1 $\mu\text{m}$ to 10 $\mu\text{m}$
Transitional Nano-Channel	0.1 $\mu\text{m}$ to 1 $\mu\text{m}$
Nano-Channel	< 0.1 $\mu\text{m}$

Another definition for microchannels is suggested by Serizawa et al. [3]. According to Serizawa et al. [3] a channel may be called a microchannel if its Laplace constant ( $L$ ) is greater than its hydraulic diameter, where

$$L = \sqrt{\frac{\sigma}{g(\rho_l - \rho_v)}} \quad (1.1)$$

This approach shows the importance of the surface tension and gravitational forces in the classification.

Moreover, Kew and Cornwell [4] suggest a confinement number ( $Co$ ) for the classification of the channels, where

$$Co = \frac{\sqrt{\frac{\sigma}{g(\rho_l - \rho_v)}}}{D_h}. \quad (1.2)$$

The confinement number can also be expressed in terms of the Laplace constant as

$$Co = \frac{L}{D_h}. \quad (1.3)$$

The confinement number should be greater than 0.5 to classify a channel as microchannel.

Different limits for the channel classification have been reported by different researchers. For example, for the flow of R-134A at 1500 kPa, the channel may be called a microchannel if  $D_h < 0.66$  mm [3], or  $D_h < 1.32$  mm [4].

The channels of the condenser and the evaporator designed in the present study have hydraulic diameters of 0.5 mm and 0.44 mm; respectively. Hence, they can be considered as microchannels [3,4].

### **1.3.2 History of Micro VCRC**

The name “micro” is due to the channel hydraulic diameters of the condenser and the evaporator in a VCRC. Therefore, it may be more meaningful to give a brief summary of the studies on the condensation and evaporation in microchannels before proceeding any further. Then, a review of the literature on the complete cycle will be presented.

### 1.3.2.1 Literature on Evaporation in Microchannels

Evaporation in microchannels has been a popular topic for about three decades, and there is a very wide literature on the subject. Due to spacing considerations, only the studies with R-134A will be mentioned in this chapter with the exception of the very first study by Lazarek and Black [5] who investigated a circular microchannel with a hydraulic diameter of 3.1 mm and length of 123 mm, with R-113 as the refrigerant. This work may be considered as the major milestone of evaporation research in miniature channels.

Yan and Lin [6] presented a study with horizontal, circular channels with hydraulic diameters of 2 mm and lengths of 200 mm. R-134A with different mass fluxes have been used as the working fluid. It has been shown that the boiling heat transfer coefficient is a function of heat flux, vapor fraction and saturation temperature in microchannels. Moreover, it is claimed that in low heat dissipation studies, the boiling heat transfer is only a function of the mass flux.

Agostini and Bontemps [7] showed the relationship between the boiling heat transfer and hydraulic diameter for vertical and rectangular channels.

Owhaib and Palm [8] studied heat transfer in vertical and circular channels of 0.8 mm, 1.2 mm and 1.7 mm hydraulic diameter, and 220 mm length. Different mass flux values have been considered in this study for a saturation temperature of 24°C. The dependency of boiling heat transfer on heat flux has been reported. Interestingly, it is stated that the heat transfer coefficient is independent of the mass flux and vapor fraction, which is in contradiction with the study of Yan and Lin [6].

Owhaib et al. [9] claimed the independency of the heat transfer coefficient from the mass flux and the vapor fraction, and highlighted the relationship between hydraulic diameter and the heat transfer coefficient.

The work of Mehendale and Jacobi [10] is another example of the heat transfer studies on microchannels where circular channels with 0.8 mm hydraulic diameter and 7.4 mm length have been considered. The claim of their study was that the boiling heat transfer coefficient is independent of the vapor fraction and the mass flux, but strongly dependent on the heat flux. Also, the dominance of the nucleate pool boiling regime has been indicated.

Huo et al. [11] presented a study with a 2.01 mm diameter and 4.06 mm length circular channel. The heat transfer coefficient has been shown to be a function of the heat flux and the vapor fraction as opposed to the findings of Owhaib et al. [9] and Mehendale and Jacobi [10]. The effect of convective boiling is not neglected in this study.

The research by Kandlikar and Steinke [12] and Kandlikar and Balasubramanian [13] may be considered among the most important studies where the correlation of boiling heat transfer coefficient in microchannels has been given in terms of the liquid phase Reynolds number. The dominance of the nucleate boiling or convective boiling regimes has been taken into account in these two studies.

### **1.3.2.2 Literature on Condensation in Microchannels**

Condensation in microchannels has been studied more recently compared to the evaporation studies in literature. Again, only the studies with R-134A will be included here.

One of the first studies on condensation in mini-channels is by Friedel [14]. The study is applicable to channels with a hydraulic diameter greater than 4 mm and it forms a bases of most for the microchannel condensation studies even at the present time. About 25000 data have been used in this study, and a pressure drop model for mini-channel condensation flow has been tried to be built up. The

separated model has been used based on a two-phase multiplier. The surface tension effects have been included in the pressure drop correlations.

Wilson et al. [15] investigated the effect of channel shape on pressure drop. The smallest channel hydraulic diameter used in this study was 1.84 mm. It has been reported that the pressure drop increases if the profile of the channel is rectangular rather than circular.

Zhang and Webb [16] investigated channels with a hydraulic diameter of 2.13 mm and reported that the work of Friedel [14] becomes inadequate in smaller channels. Still using the separated model, they developed a new two-phase multiplier.

Yang and Webb [17] studied channels with 1.41 mm hydraulic diameter. The surface tension contribution is the major point of their work. The condensation heat transfer coefficient has been given as a function of the surface tension.

Koyama et al. [18] presented a study with horizontal tubes. A saturation temperature of 60°C has been selected in their study. Based on the separated model, a newly defined two-phase multiplier has been built up.

Shin and Kim [19] highlighted that the heat transfer coefficient in square channels is higher than that in circular channels at low mass fluxes, whereas, the opposite is true at high heat fluxes. Square and circular channels with hydraulic diameters ranging between 0.5 mm and 1 mm have been used in this study.

### **1.3.2.3 Literature on Micro VCRC**

A few studies which may be considered as the milestones of the micro VCRC analyses will be given here.

Chow et al. [20] designed a meso-scale VCRC using R-134A as the refrigerant with 0.271 g/s flow rate. An evaporator heat load of 32 W has been obtained. The evaporation temperature was 12°C and the ambient temperature was 45°C. In the study, a centrifugal compressor has been used with a pressure ratio of 3.80 and a power requirement of 9.57 W, thus, a COP value of 3.34 has been reached.

In the work of Heydari [21], all components of the system were designed one by one and the refrigerator was called a miniature CPU cooling system. R-134A was used as the refrigerant. The evaporation temperature was 20°C and condensation temperature was 60°C. The condenser was designed as a compact air-cooled heat exchanger. The junction temperature was assumed to be 86°C. A positive displacement, piston-type compressor was used and the stimulation of the piston was obtained by an electrical motor instead of a crank mechanism. An isentropic compressor has been used, and the pressure lost in the valves and the manifolds have been neglected. In addition, the need for a piston-free linear vapor compression compressor has been demonstrated, and a COP value of 3.0 has been reached.

Phelan et al. [22] studied a meso-scale VCRC using R-134A. A heat load of 100-300W has been removed by the evaporator. The evaporation temperature was 5°C and the condensation temperature was 55°C. A scroll type compressor was used and a COP value of 3.0 was reached. To show the effect of the refrigerant selection on the COP value of the system, NH<sub>3</sub> and R22 were examined too. Moreover, the efficiencies of reciprocating, screw, rotary, scroll and centrifugal type compressors have been contrasted. For a range of evaporator heat loads, the geometrical details of the condenser and the compressor were given. For a 100 W load, 0.824 g/s refrigerant mass flow rate was reported to be needed and for a 300W this value has changed to 2.47 g/s. The design of the evaporator has been left as a future work in this study.

Later, Chriac and Chriac [23] designed a system for about 100 W and designed the evaporator as well. Condensation temperature has been selected as 55°C and the evaporation temperature was 10°C. R-134A has been used as the refrigerant. A scroll type compressor with a diameter of 15.2 cm and height of 15.4 cm has been selected. The COP value was 4.5.

Mongia et al. [24] designed a VCRC that may be used in Notebooks. Using R600A with 0.26 g/s mass flow rate. A heat load of 50 W has been rejected from the hot surface. The condensation temperature and the pressure were 90°C and 16.4 bar, respectively. The evaporation temperature and the pressure were 50°C and 6.85 bar, respectively. The ambient temperature was assumed to be 50°C. A reciprocating compressor with 2.4:1 pressure ratio was used and the COP value of the system was around 2.25.

#### **1.4 The Objective of the Study**

The aim of this study is to design the components of a micro VCRC one by one and to analyze the cycle. The effect of miniaturization on the pressure drop and the heat transfer in condensation and evaporation processes has been investigated. Moreover, an isentropic, reciprocating compressor has been designed for the system. Two alternative evaporator designs with different geometries have been suggested. The effect of polytropic compression process on the cycle COP has also been observed. A second law analysis has been performed at the end of the study. R-134A has been considered as the refrigerant throughout the study.

Firstly, the evaporator design part will be presented in the thesis. The design criteria and the dimensions of the evaporator will be mentioned in Chapter 2. After that, compressor design part will be discussed in Chapter 3. Chapter 4 is about the condenser design where air flow thorough the condenser fins and refrigerant flow inside the tubes will be considered. The tube and fin geometries and the dimensions will be given including their detailed calculations. Capillary

tube design will be presented in Chapter 5. The sizing of the capillary tube will be presented in this chapter. Following the design of all four components, a second law analysis will be performed in Chapter 6. The details of the code developed to analyze the system will be given in Chapter 7. The results will be presented in Chapter 8. Finally, discussions on the results, conclusions, and the potential future work will be outlined in Chapter 9.

## CHAPTER 2

### EVAPORATOR DESIGN

#### 2.1 Geometry and Material Selection

Evaporator is the component of the refrigeration system where the heat dissipated from a hot medium is removed. In this study, the evaporator is designed to be in direct contact with the heat dissipating unit. The isometric and cross-sectional views of the evaporator are presented in Figures 2.1 and 2.2, respectively. The refrigerant evaporates inside the rectangular microchannels. The dimensions of the evaporator are listed in Table 2.1

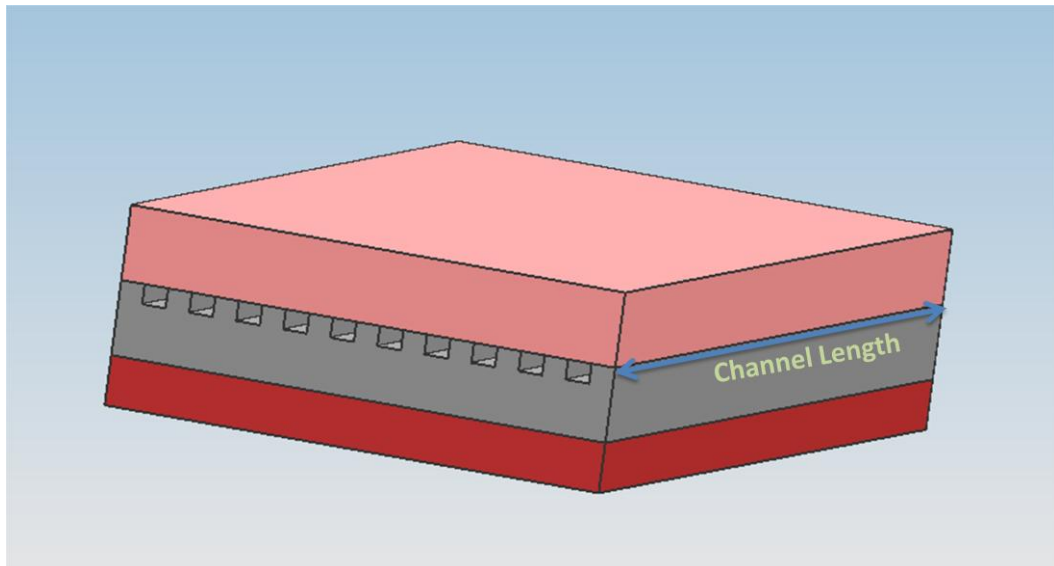


**Figure 2. 1** Isometric View of the Evaporator

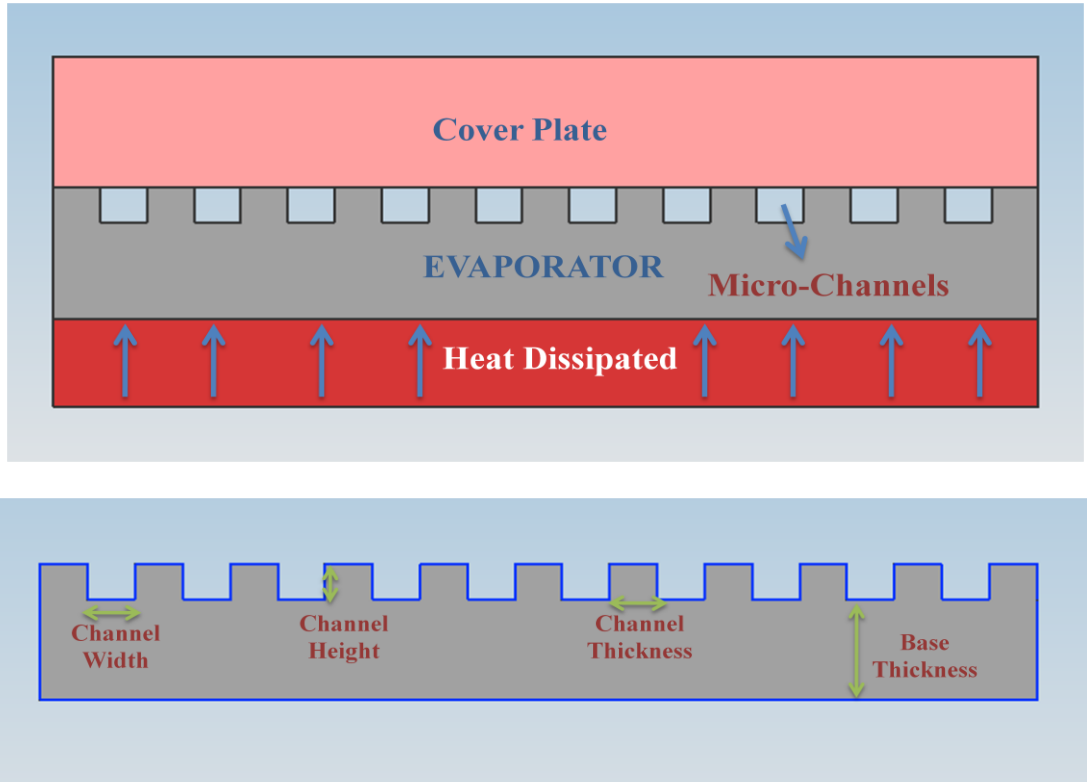


**Figure 2. 2** Evaporator Assembly

**Table 2. 1** Principle Dimensions of the Evaporator

<b>Evaporator Dimensions</b>	
Channel Height (mm)	0.400
Channel Width (mm)	0.500
Channel Thickness (mm)	0.500
Number of Channels	10
Length (mm)	18.4
Base Thickness (mm)	1

The flow area of the evaporator is given by the relation

$$A_{flow} = N H w \quad (2.1)$$

The wetted perimeter of the evaporator is

$$P = 2 N (H + w) \quad (2.2)$$

and the hydraulic diameter is

$$D_h = 4 \frac{A_{flow}}{P} \quad (2.3)$$

To reduce the thermal resistance between the hot surface and the refrigerant, copper is selected as the evaporator material due to its high thermal conductivity. The relative ease of fabrication is also considered in this selection.

## 2.2 Operational Conditions

The refrigerant enters the evaporator in the two-phase region and leaves as a superheated vapor. The operational conditions of the evaporator are summarized in Table 2.2.

**Table 2. 2** Operational Conditions of the Evaporator

<b>Inlet Vapor Fraction</b>	0.3603	<b>Cold Room Temperature (°C)</b>	15
<b>Exit Condition</b>	Superheated Vapor	<b>Boiling Pressure (MPa)</b>	0.29269
<b>Exit Temperature (°C)</b>	3	<b>Total Heat Dissipated (W)</b>	45
<b>Boiling Temperature (°C)</b>	0		

## 2.3 Heat Transfer and Pressure Drop Calculations

There are two different flow regions in the evaporator, the two-phase mixture in the entry and the superheated vapor region at the exit. Hence, the evaporator is designed and simulated for these two regions separately.

### 2.3.1 Two Phase Flow

The Reynolds numbers based on the liquid and vapor phases should be evaluated first. The liquid phase Reynolds number is as

$$Re_l = G D_h \frac{1 - x}{\mu_l} \quad (2.4)$$

and the vapor phase Reynolds number may be obtained from the relation

$$Re_v = G D_h \frac{x}{\mu_v} \quad (2.5)$$

where  $G$  is the refrigerant mass flux defined as

$$G = \frac{\dot{m}}{A_{flow}}. \quad (2.6)$$

Two types of pressure losses occur in microchannels: the frictional and accelerational. The frictional pressure drop is defined as [25]

$$\frac{\Delta P_f}{L} = \frac{\Delta P_l}{L} \phi_l^2 \quad (2.7)$$

where  $\frac{\Delta P_l}{L}$  is the liquid phase pressure drop per unit length and is given by

$$\frac{\Delta P_l}{L} = \frac{2 f_l G^2 (1 - x)^2}{D_h \rho_l}. \quad (2.8)$$

The vapor phase pressure drop may be found as

$$\frac{\Delta P_v}{L} = \frac{2 f_v G^2 x^2}{D_h \rho_v} \quad (2.9)$$

where  $f_l$  and  $f_v$  are the liquid and vapor phase friction factors which may be found for laminar flow as [26]

$$f_l = \frac{Po}{Re_l}, \quad (2.10)$$

$$f_v = \frac{Po}{Re_v} \quad (2.11)$$

respectively. The Poiseuille number is defined for rectangular channels as [27]

$$Po = 24 \left( 1 - (1.3553 a_c) + (1.9467 a_c^2) - (1.7012 a_c^3) + (0.9564 a_c^4) - (0.2537 a_c^5) \right) \quad (2.12)$$

where  $a_c$  is the aspect ratio defined as the ratio of short side of the channel to the long side [27].

Almost always, laminar flow regime develops for the liquid phase flow in microchannels. For the vapor phase, if the flow is turbulent, then the friction factor may be found as

$$f_v = (1.82 \log(Re_v) - 1.64)^{-2}. \quad (2.13)$$

The two phase pressure drop multiplier is defined as

$$\phi_l^2 = 1 + \left( \frac{C}{X} \right) + \left( \frac{1}{X^2} \right). \quad (2.14)$$

The constant  $C$  for the laminar liquid and laminar vapor phase flow conditions may be obtained as [28]

$$C = 2.16 (Re_l^{0.047}) (We_l^{0.6}) \quad (2.15)$$

and for laminar liquid and turbulent vapor phase flow conditions as

$$C = 1.45 (Re_l^{0.25}) (We_l^{0.23}). \quad (2.16)$$

The Weber number based on the liquid phase flow is defined as

$$We_l = G^2 \frac{D_h}{\rho_l \sigma}. \quad (2.17)$$

It has been shown that the pressure drop is strongly dependent on the surface tension in both laminar and turbulent flows. In addition, while finding the two phase pressure multiplier, the Martinelli parameter is an important factor which is defined as

$$X = \sqrt{\frac{(\frac{\Delta P}{L})_l}{(\frac{\Delta P}{L})_v}}. \quad (2.18)$$

The heat transfer coefficient in the two phase flow may be obtained using the following equations [12, 13]

$$h_{tp} = h_{tp_{NB}} = 0.6883 Co^{-0.2} (1-x)^{0.8} h_{lo} + (1058 Bo^{0.7} (1-x)^{0.8} S h_{lo}), \quad \text{for } Re_l < 100, \quad (2.19)$$

$$h_{tp} = \max(h_{tp_{NB}}, h_{tp_{CB}}), \quad \text{for } Re_l > 100. \quad (2.20)$$

$h_{tp_{NB}}$  is the two phase heat transfer coefficient when the nucleate boiling regime is dominant and  $h_{tp_{CB}}$  is the two phase heat transfer coefficient when convective boiling regime is dominant. They are defined as

$$h_{tp_{NB}} = 0.6883 Co^{-0.2} (1-x)^{0.8} h_{lo} + 1058 Bo^{0.7} (1-x)^{0.8} S h_{lo} \quad (2.21)$$

$$h_{tpCB} = 1.136Co^{-0.9}(1-x)^{0.8}h_{lo} + 667.2Bo^{0.7}(1-x)^{0.8}Sh_{lo} \quad (2.22)$$

where the heat transfer coefficient based on the liquid phase is defined as:

For  $100 < Re_l < 1600$

$$h_{lo} = Nu_{lo} \frac{k_l}{D_h}, \quad (2.23)$$

For  $3000 < Re_l < 10^4$

$$h_{lo} = (Re_l - 1000) Pr_l \frac{f_l}{8} \frac{\frac{k_l}{D_h}}{1 + 12.7 \left( Pr_l^{\frac{2}{3}} - 1 \right) \sqrt{\frac{f_l}{8}}}, \quad (2.24)$$

For  $10^4 < Re_l < 5 \times 10^6$

$$h_{lo} = Re_l Pr_l \frac{f_l}{8} \frac{\frac{k_l}{D_h}}{1 + 12.7 \left( Pr_l^{\frac{2}{3}} - 1 \right) \sqrt{\frac{f_l}{8}}}. \quad (2.25)$$

For the transition region where  $1600 < Re_l < 3000$ , a linear interpolation may be performed to find the liquid phase heat transfer coefficient. In addition, the boiling number, the convection number and the fluid surface parameter should be known in order to evaluate the two phase heat transfer coefficient.

The boiling number is defined as

$$Bo = \frac{q''}{G i_{lv}} \quad (2.26)$$

and the convection number which is a modified Martinelli parameter is defined as

$$Co = \left( \frac{1-x}{x} \right)^{0.8} \sqrt{\frac{\rho_v}{\rho_l}}. \quad (2.27)$$

$S$  is the fluid surface parameter for R-134A, and is given as [25]

$$S = 1.63. \quad (2.28)$$

It should be noted that, for the Reynolds number range of  $100 < Re_l < 1600$ , the Nusselt number for liquid phase is unknown, and should be found using Table 2.3 [29]. In this case, the aspect ratio  $a_c$  is defined as the ratio of the unheated side to the heated side for rectangular channels.

**Table 2.3** Nusselt Number Values for Rectangular Ducts [29]

$a_c=a/b$	<b>Nu</b>	$a_c=a/b$	<b>Nu</b>
0	8.235	1.43	3.195
0.10	6.939	2.00	3.146
0.20	6.072	2.50	3.169
0.30	5.393	3.33	3.306
0.40	4.885	5.00	3.636
0.50	4.505	10.00	4.252
0.70	3.991	>10.00	5.385
1.00	3.556		

In addition to the frictional pressure drop, there occurs an accelerational pressure drop in the two-phase region which may be found as

$$\Delta P_{acc} = G^2 \vartheta_{lv} (x_2 - x_1) \quad (2.29)$$

The total pressure drop is the sum of the frictional and accelerational pressure drops.

### 2.3.2 Single Phase Flow

The single phase flow Reynolds number is defined as

$$Re = G \frac{D_h}{\mu_{sp}}. \quad (2.30)$$

For turbulent flow, Nusselt number is given by Gnielinski as [30]

$$Nu_{GN} = \left(\frac{f}{8}\right) (Re - 1000) \frac{Pr_{sp}}{1 + 12.7 \sqrt{\frac{f}{8}} \left(Pr_{sp}^{\frac{2}{3}} - 1\right)} \quad (2.31)$$

where  $f$  is the friction factor and defined by Filonenko as [31]

$$f = (1.82 \log(Re) - 1.64)^{-2}. \quad (2.32)$$

The Nusselt number is corrected for  $2600 < Re < 23000$  and  $0.102 \text{ mm} < D_h < 1.09 \text{ mm}$  as [32]

$$Nu = Nu_{GN} (1 + F) \quad (2.33)$$

where  $F$  is defined as

$$F = C Re \left(1 - \left(\frac{D_h}{D_o}\right)^2\right) \quad (2.34)$$

and the constants  $C$  and  $D_o$  are found by a least square fit as [32]

$$D_o = 1.164 \times 10^{-3} \text{ m} \quad (2.35)$$

$$C = 7.6 \times 10^{-5}. \quad (2.36)$$

Then, the single phase heat transfer coefficient may be found using the definition

$$h = Nu \frac{k_{sp}}{D_h} \quad (2.37)$$

and the single phase pressure drop may be evaluated by the relation

$$\Delta P = f \left( \frac{1}{2} \right) \rho_{sp} U m_{sp}^2 \left( \frac{L}{D_h} \right). \quad (2.38)$$

### 2.3.3 Fin Analysis

It should be noted that the thermal resistance between the heat dissipating surface and the channel inner surface is tried to be minimized. The base temperature,  $T_b$ , of the channel may be found as

$$T_b = T_{CR} - \left( q'' \frac{t_b}{k_{cu}} \right). \quad (2.39)$$

The channels behave as fins at same time. For a fin with an insulated tip, the fin efficiency is given as [33]

$$\tau_{fin} = \frac{\tanh(m_{fin} L_c)}{m_{fin} L_c} \quad (2.40)$$

where

$$L_c = H \quad (2.41)$$

and

$$m_{fin} = \left( 2 \frac{h}{k_{Cu} t_{ch}} \right)^{0.5}. \quad (2.42)$$

Once the fin efficiency is determined, the evaporator length may be calculated as

$$L = \frac{q}{h_{tp} (2 H \eta_{fin} + t_{ch}) N \Delta T} \quad (2.43)$$

where  $\Delta T$  is the temperature difference between the channel base temperature and the boiling temperature,  $T$  :

$$\Delta T = T_b - T . \quad (2.44)$$

The calculations begin with an initial guess for the evaporator length. Hence, its accuracy should be checked at the end of the calculations. The error between the calculated and the assumed lengths, which may be calculated as

$$\% \text{ error}_L = \frac{L_{\text{calculated}} - L_{\text{initial}}}{L_{\text{initial}}} \times 100 \quad (2.45)$$

is kept within %1.

## 2.4 Alternative Evaporator Design

For the purpose of comparison, an alternative evaporator design is also suggested. The alternative evaporator has circular tubes as shown in Figure 2.3, and is designed to yield the same pressure drop as the original one. The geometrical details of the alternative evaporator are given in Table 8.2. The number and diameter of the tubes are selected iteratively to obtain the same design requirements, such as, the heat load, pressure drop, and the inlet and exit conditions. The requirements have been met by a shorter evaporator, decreasing the occupied volume, weight and the material cost. However, some manufacturing difficulties are reported in literature [34].

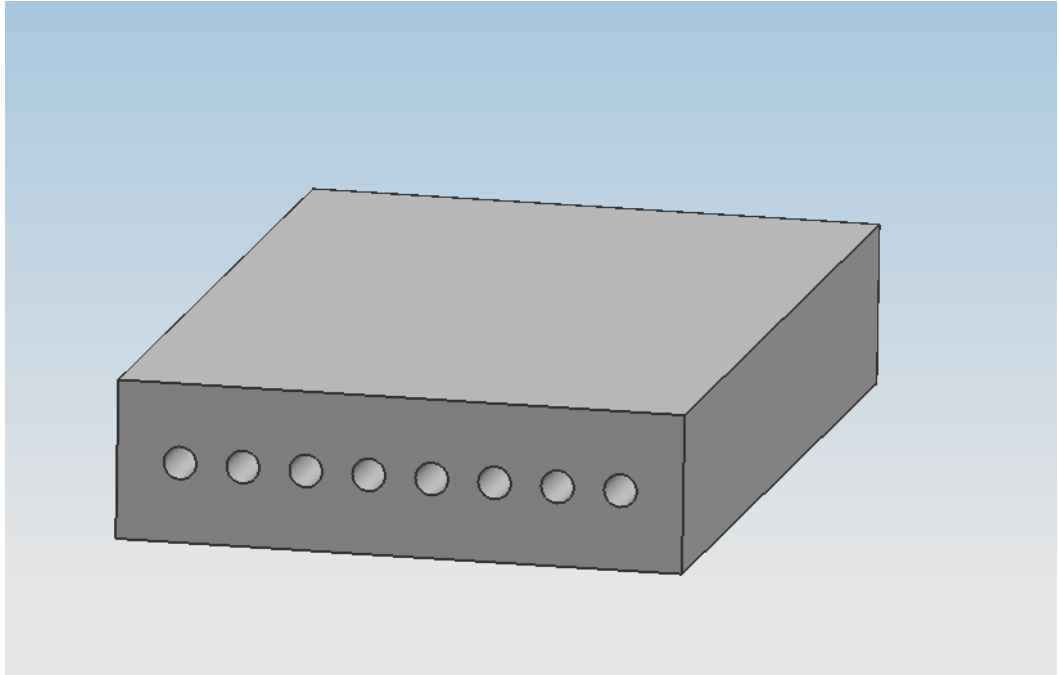


**Figure 2. 3** Alternative Evaporator

## CHAPTER 3

### COMPRESSOR DESIGN

#### 3.1 General

The function of the compressor in the vapor compression refrigeration cycle is to compress the low-pressure superheated vapor leaving the evaporator to the high-pressure condenser inlet state. In this study, a reciprocating type, isentropic compressor is designed.

#### 3.2 Principle Dimensions and Working Principles

The basic geometry and the pressure vs. volume diagram of the compressor may be seen in Figures 3.1 and 3.2. There are four stages of a reciprocating compressor:

1→2 Compression

2→3 Discharge

3→4 Re-expansion

4→1 Suction

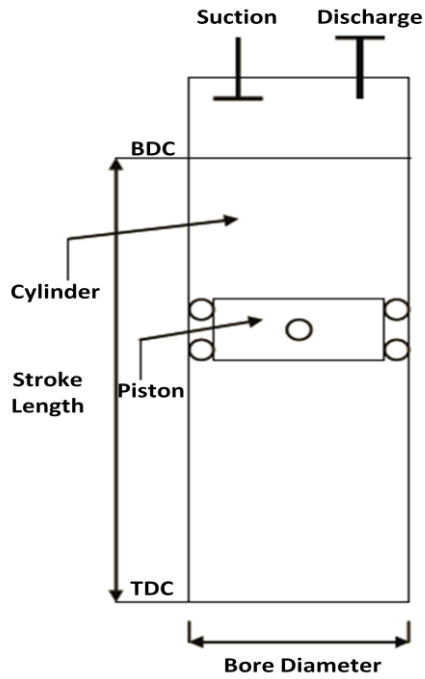


**Figure 3. 1** Basic Geometry of Compressor

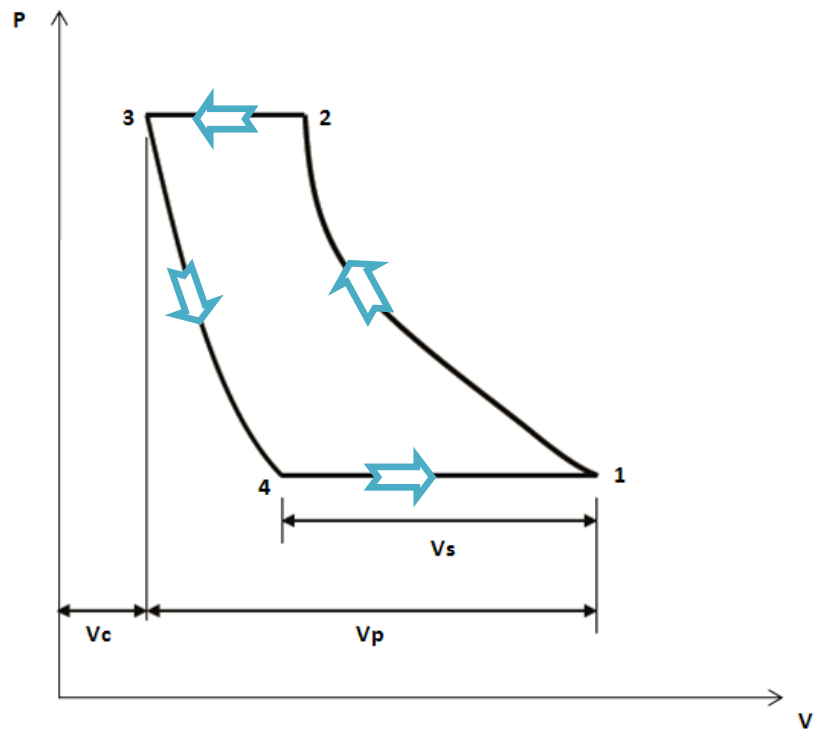


**Figure 3. 2** Pressure vs. Volume Diagram

To find the swept volume ( $V_p$ ), the suction volume ( $V_s$ ) and the clearance volume ( $V_c$ ), the ratio of the bore diameter ( $D$ ) to the stroke ( $L_{st}$ ) of the reciprocating compressor should be known firstly. Swept volume is the volume between the bottom dead center (BDC) and the top dead center (TDC), and may be calculated as

$$V_p = V_1 - V_3 = \pi \frac{D^2}{4} L_{st} . \quad (3.1)$$

The suction volume is the volume swept during the suction process and may be found as

$$V_s = V_1 - V_4 . \quad (3.2)$$

To prevent the impact of the piston on the cylinder, the cylinder is designed to have a clearance volume beyond the BDC. The clearance volume is calculated as

$$V_c = V_3 = C V_p \quad (3.3)$$

where  $C$  is defined as the clearance factor which is given as 5% regardless of the size of the compressor [35].

In real compressors, the suction and discharge pressures deviate from those seen in Figure 3.2. Due to the valve pressure drop effects, suction pressure is lower than the evaporator pressure and the discharge pressure is higher than the condenser pressure. The suction and discharge pressures may be calculated using (3.4) and (3.5), respectively,

$$P_s = P_1 f_{ps} \quad (3.4)$$

$$P_d = \frac{P_2}{f_{pd}} \quad (3.5)$$

where the pressure fractions  $f_{ps}$  and  $f_{pd}$  at the suction and discharge valves are given as [35]

$$f_{ps} = 0.95 \quad (3.6)$$

$$f_{pd} = 0.95 \quad (3.7)$$

The effect of the valve pressure drops may be seen in Figure 3.3.

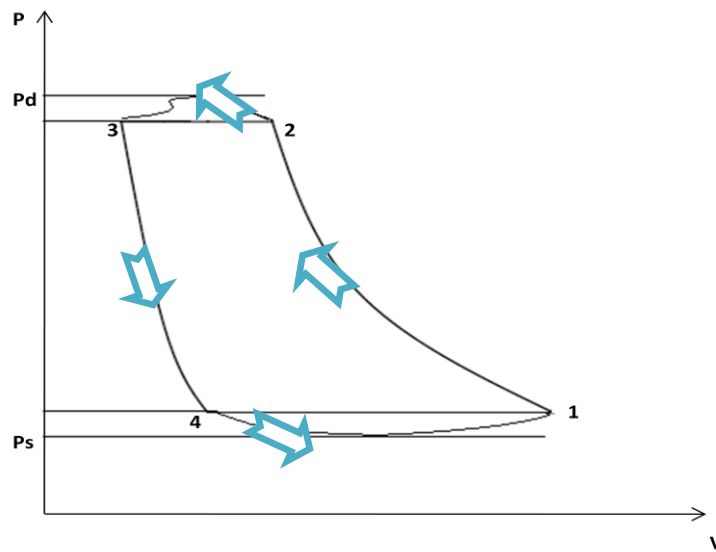


**Figure 3.3** Suction and Discharge Pressures

### 3.3 Compressor Work

The power input to the compressor may be found from Figure 1.4 as the product of the mass flow rate and the difference between evaporator exit and condenser inlet specific enthalpies

$$W = \dot{m} (i_1 - i_4). \quad (3.8)$$

The specific work of the compressor may be calculated as

$$w = \oint v dP. \quad (3.9)$$

For this study, for an isentropic compression and isentropic re-expansion process, the specific work of the compressor is defined as [35]

$$w_{comp} = \left( \frac{k}{k-1} \right) P_1 v_1 \left( \left( \frac{P_d}{P_l} \right)^{\frac{k-1}{k}} - 1 \right) \quad (3.10)$$

where  $k$  is the isentropic index of compression. From the ideal gas relation,

$$P v^k = P_1 v_1^k = P_2 v_2^k = \text{CONSTANT} \quad (3.11)$$

and

$$k = \frac{\ln \left( \frac{P_2}{P_1} \right)}{\ln \left( \frac{v_1}{v_2} \right)}. \quad (3.12)$$

Therefore, it is nearly the ratio of the constant pressure specific heat to the constant volume specific heat

$$k \cong \frac{c_p}{c_v}. \quad (3.13)$$

The power input to the compressor may be calculated by multiplying the specific work with the mass flow rate of the refrigerant

$$W_{comp} = \dot{m} w_{comp}. \quad (3.14)$$

### 3.4 Compressor Performance

There are different performance definitions for the compressor. In this study, the compressor is selected as isentropic. Therefore, the isentropic efficiency, which is the ratio of the isentropic work to the actual work is unity.

$$\eta_{isent.} = \frac{W_{isent.}}{W_{actual}} \quad (3.15)$$

In a reciprocating compressor, the ratio of suction volume to swept volume is defined as the clearance volumetric efficiency, which may be found as [35]

$$\eta_{cl.} = \frac{V_s}{V_p} = 1 + C - C \left( \frac{P_d}{P_s} \right)^{\frac{1}{k}} \quad (3.16)$$

where  $C$  was defined as the clearance factor. The most commonly used term for the efficiency in a reciprocating compressor is the overall volumetric efficiency that can be found from [35]

$$\eta_{vol.} = (1 + C) \left( \frac{P_s}{P_1} \right)^{\frac{1}{k}} - C * \left( \frac{P_d}{P_1} \right)^{\frac{1}{k}} - f_{leakage} \left( \frac{P_d}{P_s} \right) \quad (3.17)$$

where  $f_{leakage}$  is assumed as 0.01.

### 3.5 Compressor Speed

The rotational speed of the compressor may be found as

$$N_{comp.} = \frac{\dot{m} v_1}{\eta_{vol} V_p} \times 60 \quad (3.18)$$

and the mean velocity of the piston is

$$U_{m_{piston}} = 2 L \frac{N_{comp.}}{60} \quad (3.19)$$

where  $N_{comp.}$  is in rpm and  $U_{m_{piston}}$  is in m/s.

## CHAPTER 4

### CONDENSER DESIGN

#### 4.1 Geometry and Material

The condenser is designed as an air-cooled, micro-channel, multi-louver fin heat exchanger. The basic geometry of the microchannel condenser is given in Figure 4.1 and the louvered-fin geometry is presented in Figure 4.2.

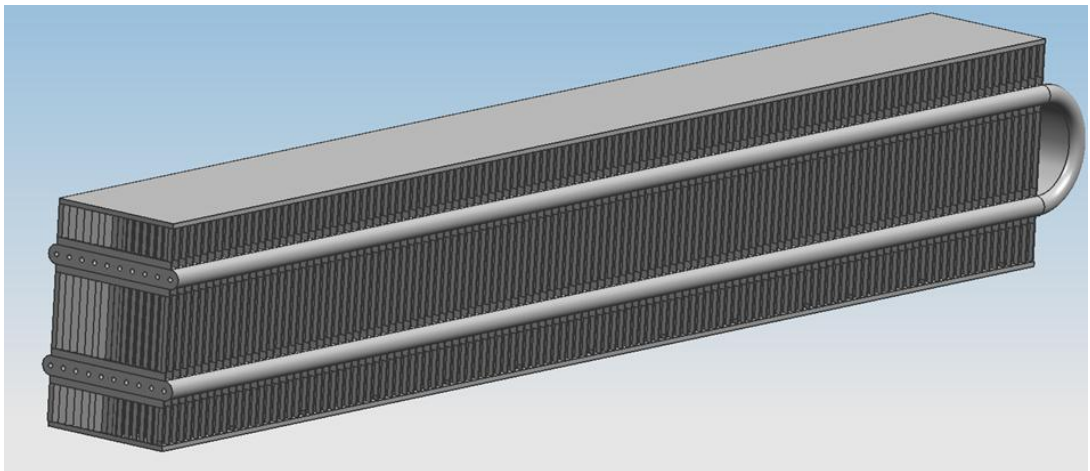


**Figure 4. 1** Condenser Geometry

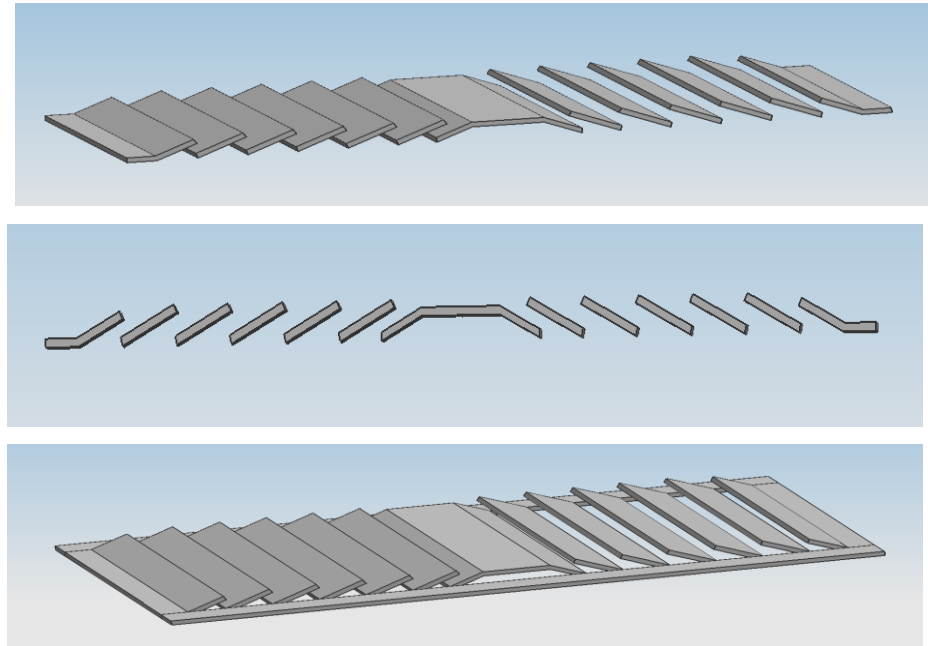


**Figure 4. 2** Fin Geometry

Additionally, geometrical details of the condenser and the louvered fins are shown in Table 4.1 and Figure 4.3.

**Table 4. 1** Principle Dimensions

Tube Side		Fin Side		Louver	
Tube Height (mm)	1.96	Fin Pitch (mm)	1.114	Louver Angle (°)	27
Tube Depth (mm)	16.26	Fin Length (mm)	9.15	Louver Pitch (mm)	0.94
Number of Channels	10	Fin Thickness (mm)	0.127	Louver Length (mm)	7.62
Channel Diameter (mm)	0.5				
Length (mm)	135				

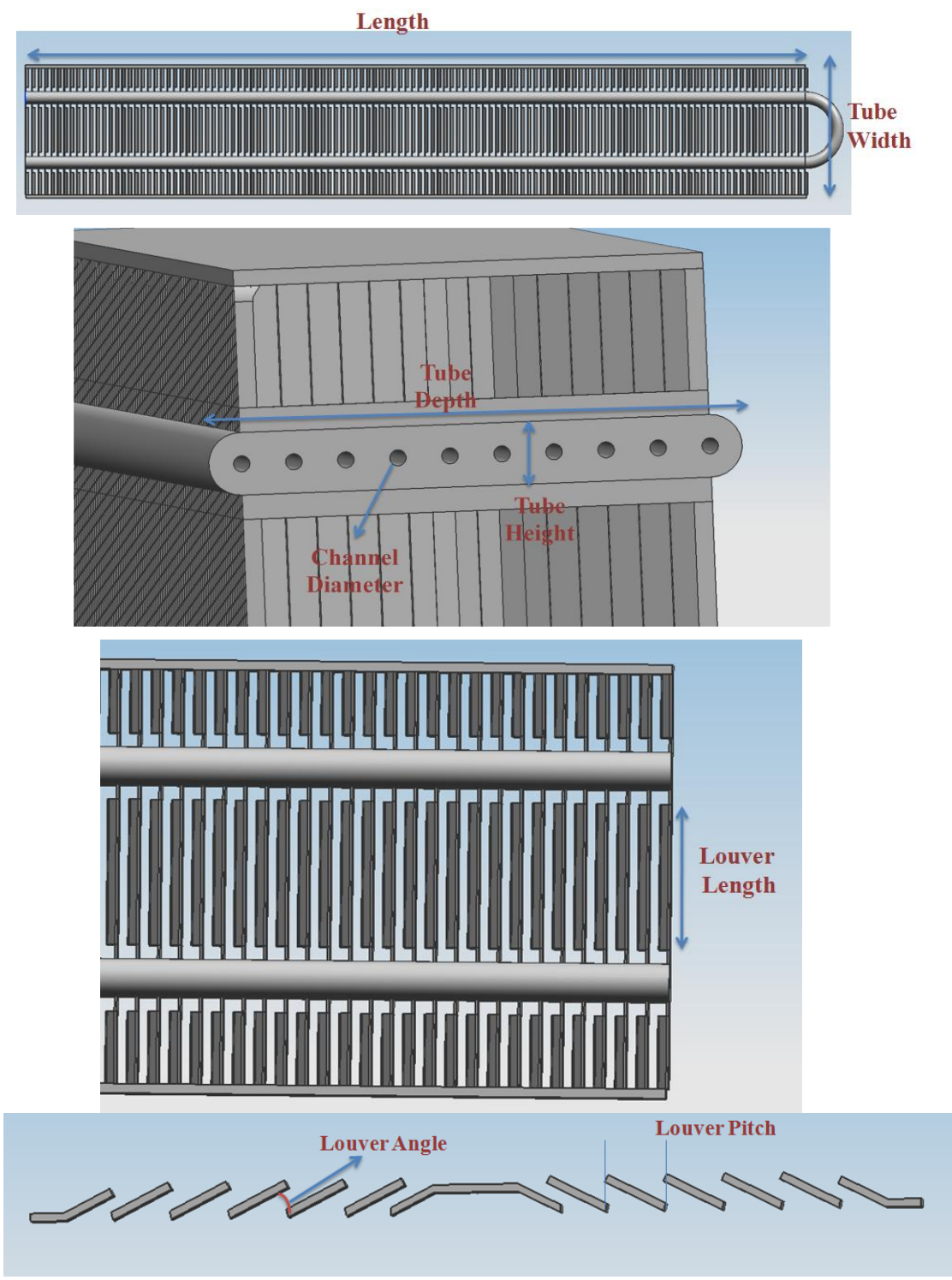


**Figure 4. 3** Principle Dimensions of Condenser

The flow area of the refrigerant side of the condenser is given by

$$A_{flow} = N \pi \frac{D^2}{4}. \quad (4.1)$$

The wetted perimeter of the refrigerant channels is

$$P = N \pi D \quad (4.2)$$

and the hydraulic diameter is

$$D_h = 4 \frac{A_{flow}}{P}. \quad (4.3)$$

The free flow area for the air side of the condenser is given by

$$A_{free_a} = (L_{seg} - N_{fin} z_t) z_l. \quad (4.4)$$

For the air side, the wetted perimeter is

$$P_a = 4 \left( L_{seg} - N_{fin} z_t + \frac{z_l}{2} \right) \quad (4.5)$$

and the hydraulic diameter of air side is

$$D_{ha} = 4 \frac{A_{free_a}}{P_a}. \quad (4.6)$$

As an alternative to copper which was used for the evaporator, aluminum is selected for both the air and the refrigerant sides of the condenser, due to its lower density and cost, as well as the availability of empirical correlations.

## 4.2 Operational Conditions

The operational conditions of the condenser are stated in Table 4.2.

**Table 4. 2** Design Variables of the Condenser

Refrigerant Side		Air Side	
Refrigerant Mass Flow Rate (g/s)	0.35	Air Mass Flux (kg/m <sup>2</sup> s)	5
Refrigerant Inlet Pressure (MPa)	1.3177	Air Inlet Temperature (°C)	30
Refrigerant Inlet Temperature (°C)	58.05		
Refrigerant Condensation Temperature (°C)	50		

## 4.3 Calculation Scheme

The air-cooled condenser is where the heat rejection from the system takes place. The refrigerant enters the condenser as a super-heated vapor and exits as a sub-cooled or saturated liquid. Calculations are performed for the single phase and two-phase regions separately. In the superheated region, the flow is in single-phase and the refrigerant properties vary along the tube length with varying temperature. On the other hand, in the condensation region, the refrigerant is in two-phase and its properties vary along the tube length with varying refrigerant quality. In order to minimize the calculation errors due to the mentioned property variations, the tube is divided into segments. The number of segments is determined based on the heat transfer and pressure drop correlations. Four segments are used in the two-phase flow region and one segment is used in the single phase flow region.

For the single phase region, the refrigerant properties at the inlet of the first segment are the same as those of the super-heated vapor leaving the compressor. For two-phase region, the first segment properties are saturated vapor properties nearly at the same pressure as the saturated vapor but at a lower temperature. For all segments, the refrigerant properties are evaluated as the arithmetic average of the inlet and exit properties. However, since the exit properties of a segment cannot be known at the beginning, an initial assumption should be made first, and an iterative procedure should be followed. Finding the enthalpy loss and pressure drop for a segment, the outlet conditions may be found for that segment. If the difference between the assumed value and calculated value is less than 1%, calculations may continue for the next segment.

#### **4.4 Refrigerant Side Heat Transfer and Pressure Drop Calculations**

Calculations for the refrigerant side are performed in two separate regions, the single phase and the two-phase regions, respectively. Refrigerant R-134A properties are taken from ASHRAE transactions [36] and a code is written to interpolate the properties for any temperature and pressure value.

##### **4.4.1 Single Phase Flow**

For the single phase flow in refrigerant side the Reynolds number is defined as

$$Re = G \frac{D_h}{\mu_{sp}} \quad (4.7)$$

For laminar flow, assuming constant surface temperature, the Nusselt number is defined as [33]

$$Nu = 3.66 . \quad (4.8)$$

It should be noted that vapor flow in microchannels is rarely laminar.

For turbulent flow, the Nusselt number is defined by Gnielinski as [30]

$$Nu_{GN} = \left(\frac{f}{8}\right) (Re - 1000) \frac{Pr_{sp}}{1 + 12.7 \sqrt{\frac{f}{8}} \left(Pr_{sp}^{\frac{2}{3}} - 1\right)} \quad (4.9)$$

where  $f$  is the friction factor and is defined by Filonenko as [31]

$$f = (1.82 \log(Re) - 1.64)^{-2} \quad (4.10)$$

The Nusselt number is corrected for  $2600 < Re < 23000$  and  $0.102 \text{ mm} < D_h < 1.09 \text{ mm}$  [32]

$$Nu = Nu_{GN} (1 + F) \quad (4.11)$$

where  $F$  is defined as

$$F = C Re \left(1 - \left(\frac{D_h}{D_o}\right)^2\right). \quad (4.12)$$

The constants  $D_o$  and  $C$  are found by a least square fit as [32]

$$D_o = 1.164 \times 10^{-3} \text{ meters} \quad (4.13)$$

$$C = 7.6 \times 10^{-5}. \quad (4.14)$$

The single phase heat transfer coefficient is defined as

$$h = Nu \frac{k_{sp}}{D_h} \quad (4.15)$$

and the single phase pressure drop may be calculated as

$$\Delta P = f \left(\frac{1}{2}\right) \rho_{sp} U m_{sp}^2 \left(\frac{L}{D_h}\right). \quad (4.16)$$

#### 4.4.2 Two Phase Flow

For the two-phase flow part, the sum of the frictional and decelerational pressure drops may be found using the relation given by Garimella as [37]

$$\Delta P = \left(\frac{1}{2}\right) f_i G^2 \frac{x^2}{\rho_v * \alpha_v^{2.5}} \frac{L}{D_h} \quad (4.17)$$

where  $f_i$  is the interfacial friction factor given by Lee and Lee as [38]

$$f_i = A X^a Re_l^b \varphi^c f_l. \quad (4.18)$$

$\varphi$  is the surface tension parameter and is given by

$$\varphi = j_l \frac{\mu_l}{\sigma}. \quad (4.19)$$

$j_l$  is the liquid superficial velocity and may be found as

$$j_l = G \frac{1 - x}{\rho_l (1 - \alpha_v)} \quad (4.20)$$

where  $f_l$  is the liquid-phase Darcy friction factor.

For  $Re_l < 2100$

$$A = 1.308 \times 10^{-3} \quad a = 0.427 \quad b = 0.930 \\ c = -0.121 \quad f_l = \frac{64}{Re} \quad (4.21)$$

For  $Re_l > 3400$

$$A = 25.64 \quad a = 0.532 \quad b = 0.327 \quad c = 0.021 \\ f_l = 0.316 (Re_l^{-0.25}) \quad (4.22)$$

The liquid-phase and vapor-phase Reynolds numbers are defined as

$$Re_l = G D_h \frac{1 - x}{\mu_l (1 + \sqrt{a_v})} \quad (4.23)$$

$$Re_v = G D_h \frac{x}{\mu_v \sqrt{a_v}} \quad (4.24)$$

where  $a_v$  is the void fraction given by Baroczy as [39]

$$a_v = \left( 1 + \left( \frac{1 - x}{x} \right)^{0.74} \left( \frac{\rho_v}{\rho_l} \right)^{0.65} \left( \frac{\mu_l}{\mu_v} \right)^{0.13} \right)^{-1}. \quad (4.25)$$

$X$  is the Martinelli parameter defined as

$$X = \left( \frac{1 - x}{x} \right)^{0.9} \left( \frac{\rho_v}{\rho_l} \right)^{0.5} \left( \frac{\mu_l}{\mu_v} \right)^{0.1}. \quad (4.26)$$

The two-phase heat transfer coefficient is defined as [37]

$$h = \rho_l C p_l \frac{u^*}{T^+} \quad (4.27)$$

where  $u^*$  is the dimensionless friction velocity given by Garimella as [37]

$$u^* = \sqrt{\frac{\tau_i}{\rho_l}} \quad (4.28)$$

where  $\tau_i$  is the interfacial shear stress defined by Bandhauer [40] as

$$\tau_i = \left( \frac{\Delta P}{L} \right) \sqrt{a_v} \frac{D_h}{4} \quad (4.29)$$

and  $T^+$  is the turbulent dimensionless temperature defined by Garimella [37] as

For  $Re_l < 2100$

$$T^+ = 5 Pr_l + 5 \ln \left( Pr_l \left( \frac{\delta^+}{5} - 1 \right) + 1 \right) \quad (4.30)$$

For  $Re_l > 2100$

$$T^+ = 5 Pr_l + 5 \ln(Pr_l + 1) + \int_{30}^{\delta^+} dy^+ / \left( \left( \frac{1}{Pr_l} - 1 \right) + \frac{y^+}{5} \left( 1 - \frac{y^+}{R^+} \right) \right) \quad (4.31)$$

$R^+$  is the dimensionless pipe radius and is defined as

$$R^+ = R \rho_l \frac{u^*}{\mu_l} \quad (4.32)$$

and  $R$  is the pipe radius in meters.

$$y^+ = y \rho_l \frac{u^*}{\mu_l} \quad (4.33)$$

$\delta^+$  is the dimensionless turbulent film thickness defined as

$$\delta^+ = \delta \rho_l \frac{u^*}{\mu_l} \quad (4.34)$$

and  $\delta$  is the turbulent film thickness determined using [37]

$$\delta = (1 - \sqrt{a_v}) \frac{D_h}{2}. \quad (4.35)$$

In addition to the frictional and decelerational pressure drops, there occur minor pressure drops due to the bends on the refrigerant side. The pressure drop through the bends can be calculated as

$$\Delta P_{bend} = \left(\frac{1}{2}\right) k_{minor} \rho_r V_r^2 \quad (4.36)$$

where  $k_{minor}$  is the minor loss coefficients for bends and a value of 0.2 is used for the loss coefficient in this study. For the two-phase flow, the pressure drop through the bends may be calculated using the correlation given by Rohsenow et al. [41]

$$\Delta P_{bend_{two-phase}} = \Delta P_{bend_{liq}} \left(1 + \frac{2x\rho_{liq}}{\rho_r}\right). \quad (4.37)$$

The total pressure drop may be calculated by summing the frictional, decelerational and minor pressure drops at bends for the refrigerant side of the condenser.

It should be taken into consideration that the length of the single phase flow part of the condenser is a very small compared to the two-phase flow part, and is neglected in most of the studies in literature.

#### **4.5 Air-Side Heat Transfer and Pressure Drop Calculations**

Since the air temperature varies along the flow path, an iterative process is performed while evaluating the air properties. Air outlet temperature is guessed initially and the actual outlet temperature is calculated with at most 1% error. The air properties are then evaluated at the mean temperature. The air velocity is kept under 4.5 m/s in this study.

To find the air side pressure drop, a friction factor is found by Kim and Bullard as [42]

$$f_a = (Re_{lp}^{-0.781}) \left(\frac{\theta}{90}\right)^{0.444} \left(\frac{z_p}{l_p}\right)^{-1.682} \left(\frac{z_l}{l_p}\right)^{-1.22} \left(\frac{z_d}{l_p}\right)^{0.818} \left(\frac{l_l}{l_p}\right)^{1.97} \quad (4.38)$$

where  $Re_{lp}$  is the Reynold number based on louver pitch defined as

$$Re_{lp} = G_a \frac{l_p}{\mu_a}. \quad (4.39)$$

The air side pressure drop is calculated as

$$\Delta P_a = f_a G_a^2 \frac{z_d}{2 \rho_a l_p}. \quad (4.40)$$

To find the air side heat transfer coefficient, Colburn-j factor is used which is found by Chang and Wang [43] for multi-louvered fins as

$$j_{colb} = 1.18 (Re_{lp}^{-0.505}) \left(\frac{\theta}{90}\right)^{0.26} \left(\frac{z_l}{l_p}\right)^{-0.51} \left(\frac{z_d}{l_p}\right)^{-0.26} \left(\frac{l_l}{l_p}\right)^{0.82} \left(\frac{t_p}{l_p}\right)^{-0.25} \left(\frac{z_t}{l_p}\right)^{-0.097} \quad (4.41)$$

and the air side heat transfer coefficient is calculated as

$$h_a = j_{colb} C p_a \rho_a U m_a Pr_a^{-\frac{2}{3}}. \quad (4.42)$$

The power requirement of the air side fan is calculated as

$$Power = \Delta P_a \frac{\dot{m}_a}{\rho_a}. \quad (4.43)$$

#### 4.6 Overall Heat Transfer Calculations

The overall heat transfer coefficient is calculated as

$$U_o = \frac{1}{\left(\frac{A_o}{A_i h_i}\right) + \left(\frac{1}{h_a \eta_{fin_o}}\right)} \quad (4.44)$$

where  $A_o$  is the outer side heat transfer area,  $A_i$  is the inner side heat transfer area,  $h_i$  is the inner side heat transfer coefficient,  $\eta_{fin_o}$  is the overall fin efficiency defined as

$$\eta_{fin_o} = 1 - \left(\frac{A_{fin}}{A_{tot}}\right) (1 - \eta_{fin_a}) \quad (4.45)$$

and  $\eta_{fin_a}$  is the fin efficiency given by

$$\eta_{fin_a} = \frac{\tanh(m_{fin} Lc_{fin})}{m_{fin} Lc_{fin}}. \quad (4.46)$$

$m_{fin}$  and  $Lc_{fin}$  are given by [33]

$$m_{fin} = \left(2 \frac{h_a}{k_{fin} z_t}\right)^{0.5} \quad (4.47)$$

$$Lc_{fin} = (z_l) + \left(\frac{z_t}{2}\right) \quad (4.48)$$

$\epsilon$ - $NTU$  method is used to find the total heat transfer where

$$NTU = U_o \frac{A_o}{C_{min}}, \quad (4.49)$$

$$C_{min} = m_a C_{p,a}. \quad (4.50)$$

The maximum heat transfer is found by

$$q_{max} = C_{min} (T_{ri} - T_{ai}) \quad (4.51)$$

where  $T_{ri}$  is the refrigerant inlet temperature and  $T_{ai}$  is the air inlet temperature.

The condenser effectiveness is calculated using

$$\epsilon = 1 - \exp(-NTU) \quad (4.52)$$

Finally, the total heat transfer rate may be calculated as

$$q_{tot} = q_{max} \epsilon. \quad (4.53)$$

## CHAPTER 5

### CAPILLARY TUBE DESIGN

#### 5.1 Introduction

Capillary tube is one of the basic components of a vapor compression refrigeration cycle. The function of the tube is to reduce the pressure of the refrigerant from condenser pressure to the evaporator pressure. Therefore, a long, narrow tube is used. There are two basic reasons for the high-pressure drop in the tube:

- i. Since the diameter of the tube is very small and the length very long, the frictional pressure drop occurs in the tube.
- ii. The saturated liquid exiting the condenser turns into a two-phase mixture, when entering the evaporator. Since the mass flow rate of the refrigerant is constant, the density of it reduces due to the vapor formation. It leads to a higher velocity in tube and an accelerational pressure drop occurs.

The total pressure drop inside the capillary tube may be written as

$$\Delta P = \Delta P_f + \Delta P_{acc} \quad (5.1)$$

## 5.2 Sizing of the Capillary Tube

The sizing of the capillary tube is in effect selecting the length and diameter of the tube. Any different combinations of the length and diameter may give the same pressure drop in the system. There are actually two basic methods to size the tube. The first method is commonly used in mass production. After selecting the diameter and length of the hose, a hose with greater length is installed in the system. The hose is cut until the desired pressure drop is achieved. This method is called the *cut-and-try* method. The second method is used commonly for unique system designs. The length and diameter of the hose are selected and a hose which is a little shorter than the desired length is installed in the system. The desired pressure drop is then obtained by *pinching* the hose at some points.

Either using the cut-and-try method or the pinching method, the length and the tube diameter should be decided first. Hence, in the present study, the design of the capillary tube is performed by determining these two parameters.

## 5.3 Pressure Drop in the Capillary Tube

In this study, an isenthalpic capillary tube is considered. Actually, the flow in a capillary tube is three-dimensional, compressible and in two-phase. However, the analytical studies with incompressible, one-dimensional and single phase flow assumptions yield highly accurate results.

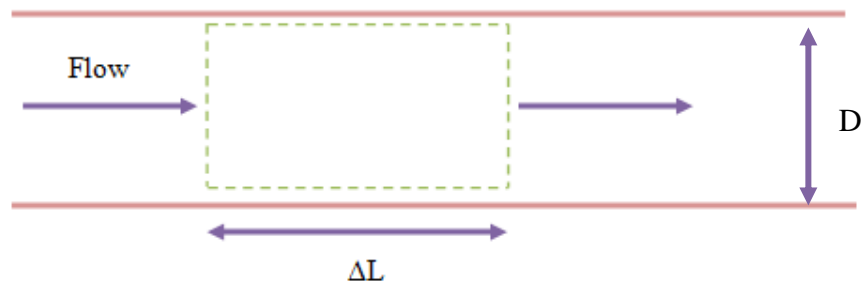


**Figure 5. 1** Capillary Tube Section

A capillary tube section is illustrated in Figure 5.1. To find the pressure drop in the section, conservation of mass and momentum equations should be solved for this control volume (CV).

Conservation of Mass:

$$\rho V A_c + \frac{\partial(\rho V)}{\partial L} \Delta L A_c - \rho V A_c = 0 \quad (5.2)$$

where

$$A_c = \frac{\pi D^2}{4} \quad (5.3)$$

thus,

$$\frac{\partial(\rho V)}{\partial L} = 0 \quad (5.4)$$

Hence,  $\rho V = \text{Constant}$

Conservation of Momentum:

$$\Sigma M_{out} - \Sigma M_{in} = \Sigma F_{CV} . \quad (5.5)$$

In other words, the difference between the momentums entering and leaving the CV is equal to the sum of the forces on the control volume. Including the gravitational force and shear forces in the equation,

$$\begin{aligned} A_c \left( \rho V^2 + \rho V \left( \frac{\partial V}{\partial L} \right) \Delta L \right) - A_c \rho V^2 \\ = -A_c \frac{\partial P}{\partial L} \Delta L - \rho_{mean} g A_c \Delta L \\ - \pi D \Delta L \tau_w \end{aligned} \quad (5.6)$$

Since  $\Delta L$  is an infinitesimal length, the gravitational force is neglected and higher order terms are diminished. Dividing both sides by  $A_c \Delta L$  as  $\Delta L$  converges to zero gives

$$\rho V \frac{\partial V}{\partial L} = -\frac{\partial P}{\partial L} - 4 \frac{\tau_w}{D} \quad (5.7)$$

Shear stress causes frictional pressure drop in the pipe and therefore, it is written in terms of the friction factor

$$\tau_w = D \frac{\Delta P_{fric}}{4 \Delta L} \quad (5.8)$$

where frictional pressure drop is calculated as

$$\Delta P_f = \rho f \left( \frac{\Delta L}{D} \right) \left( \frac{V^2}{2} \right) \quad (5.9)$$

The friction factor is defined for laminar flow ( $Re < 2300$ ) as

$$f = \frac{64}{Re} \quad (5.10)$$

For turbulent flow, the friction factor is defined by Blasius as

$$f = 0.33 Re^{-0.25} \quad (5.11)$$

for  $2300 < Re < 10^5$ . The shear stress is written as

$$\tau_w = \rho f \frac{V^2}{8}. \quad (5.12)$$

Substituting the shear stress in (5.7),

$$\rho V \frac{\partial V}{\partial L} = -\frac{\partial P}{\partial L} - \rho f \frac{V^2}{2D}. \quad (5.13)$$

Conservation of mass equation gives  $\rho V = \mathbf{constant}$ , and this constant is the mass flux which can be written as

$$\rho V = \frac{\dot{m}}{A_c} = G. \quad (5.14)$$

Substitution of G in (5.13) yields

$$G \frac{\partial V}{\partial L} = -\frac{\partial P}{\partial L} - f \frac{V G}{2D}. \quad (5.15)$$

Integration of (5.15) over the infinitesimal length  $\Delta L$  gives

$$G \Delta V = -\Delta P - \left( \left( f \frac{V G}{2D} \right)_2 - \left( f \frac{V G}{2D} \right)_1 \right) \Delta L \quad (5.16)$$

Taking the friction factor and the velocity as the average values for states 1 and 2,

$$G \Delta V = -\Delta P - (f V)_{mean} G \frac{\Delta L}{2D}. \quad (5.17)$$

The total pressure drop may be found as

$$\Delta P = G \Delta V + (f V)_{mean} G \frac{\Delta L}{2D} \quad (5.18)$$

To reduce the margin of errors in calculations, the total length of the hose is divided into segments and the total length of the hose is found as the sum of the lengths of these segments. The calculation procedure is explained next.

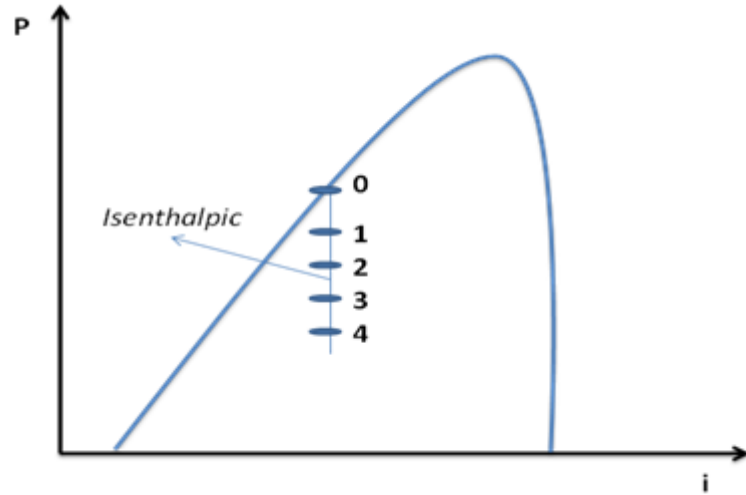


**Figure 5. 2** Segmentation in capillary tube

First, a differential temperature value should be assumed for all segments as seen in Figure 5.2. Thus,  $T_1 = T_0 - \Delta T$ . The properties of the refrigerant and friction factor are evaluated at state 0. Knowing  $T_1$ , the saturation pressure is found at state 1. Then, the liquid and vapor properties are found at state 1. However, the vapor fraction must be known to evaluate the properties. Since the process is assumed to be isenthalpic, i.e.  $i_0 = i_1$ , the enthalpy at state 1 can be written as

$$i_1 = x_1 i_{g1} + (1 - x_1) i_{f1} \quad (5.19)$$

and the vapor fraction is

$$x_1 = \frac{i_1 - i_{f1}}{i_{g1} - i_{f1}} \quad (5.20)$$

Properties at state 1 can be calculated as

$$\mu_1 = x_1 \mu_{g1} + (1 - x_1) \mu_{f1} \quad (5.21)$$

$$v_1 = x_1 v_{g1} + (1 - x_1) v_{f1} \quad (5.22)$$

At the end, the length of the hose for segment 1 is found as

$$\Delta L_1 = \frac{-\Delta P - G \Delta V}{\left(\frac{G}{2D}\right) (f V)_{mean}} \quad (5.23)$$

The total length of the hose is the sum of the lengths of all segments.

One of the most important design criteria for a capillary tube is to avoid choking. If the velocity in the tube exceeds the speed of sound, choking occurs and it is not a desired condition. Figure 5.3 shows the choked flow condition in a tube under constant condenser temperature. In case of choked flow, a capillary tube with a higher diameter should be selected.

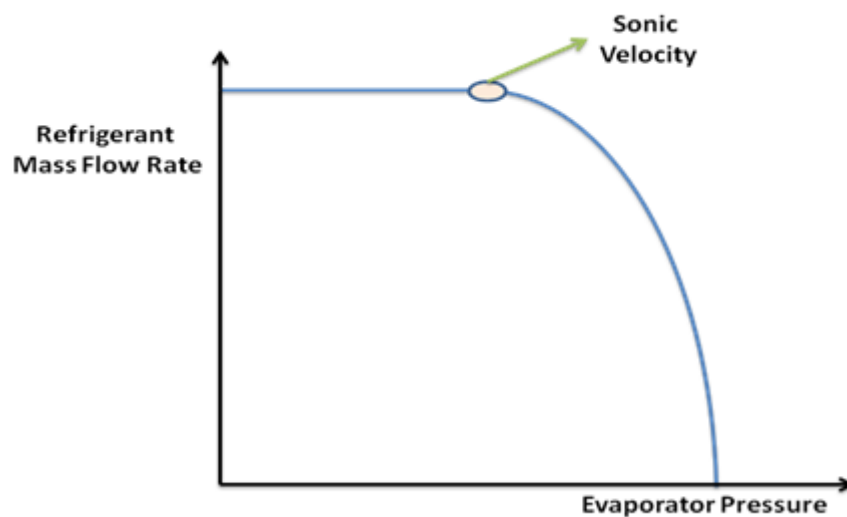


**Figure 5. 3** Choked Flow Condition

## CHAPTER 6

### SECOND LAW ANALYSIS

#### 6.1 General Considerations

To analyze a vapor compression refrigeration system based on the second law of thermodynamics is not an easy task. Moreover, in the present study, the system scale is smaller than a conventional refrigeration cycle, which is thought to cause a higher entropy generation. Sangkwon considers systems with about 10  $\mu\text{m}$  evaporator channel hydraulic diameter [44], and explains the difficulty of miniaturization of a refrigeration system in terms of the second law analysis. Although the mentioned system is much smaller compared to that of the present study, the analysis still gives an opinion about the entropy generation in small systems. Interestingly, the entropy generation in the evaporator, condenser and the capillary tube is not a function of the length scale. On the other hand, entropy generation increases with decreasing length scale of the compressor.

In this study, an isentropic compressor is used. However, to show the effect of unisentropic, a cycle with polytropic compression is simulated too. The second law analysis of the whole cycle is performed [35, 45] by calculating the irreversibilities of all components one by one and summing them to find the cycle irreversibility.

$$I_{comp} = \dot{m} T_{room} (s_2 - s_1) - Q_{comp} \quad (6.1)$$

$$I_{cond} = \dot{m} T_{room} (s_3 - s_2) - Q_{cond} \quad (6.2)$$

$$I_{capillary} = \dot{m} T_{room} (s_4 - s_1) \quad (6.3)$$

$$I_{evp} = \dot{m} T_{room} (s_1 - s_4) - Q_{evp} \frac{T_{room}}{T_{CR}} \quad (6.4)$$

$$I_{cycle} = I_{comp} + I_{cond} + I_{capillary} + I_{evp} \quad (6.5)$$

In (6.1-6.4) the room temperature and the cold room temperature are in K. The results of the second law analysis are presented in Chapter 8.

## **CHAPTER 7**

### **SIMULATIONS**

#### **7.1 General**

The complete design of a micro-scale VCRC is performed in this study. MATLAB is used as the software. The correlations used for the design of each component were given in previous chapters. In this chapter, the details of the code are presented. The design criteria and the code algorithm are also given.

#### **7.2 Algorithm**

The design algorithm of the complete cycle is given in Figure 7.1.

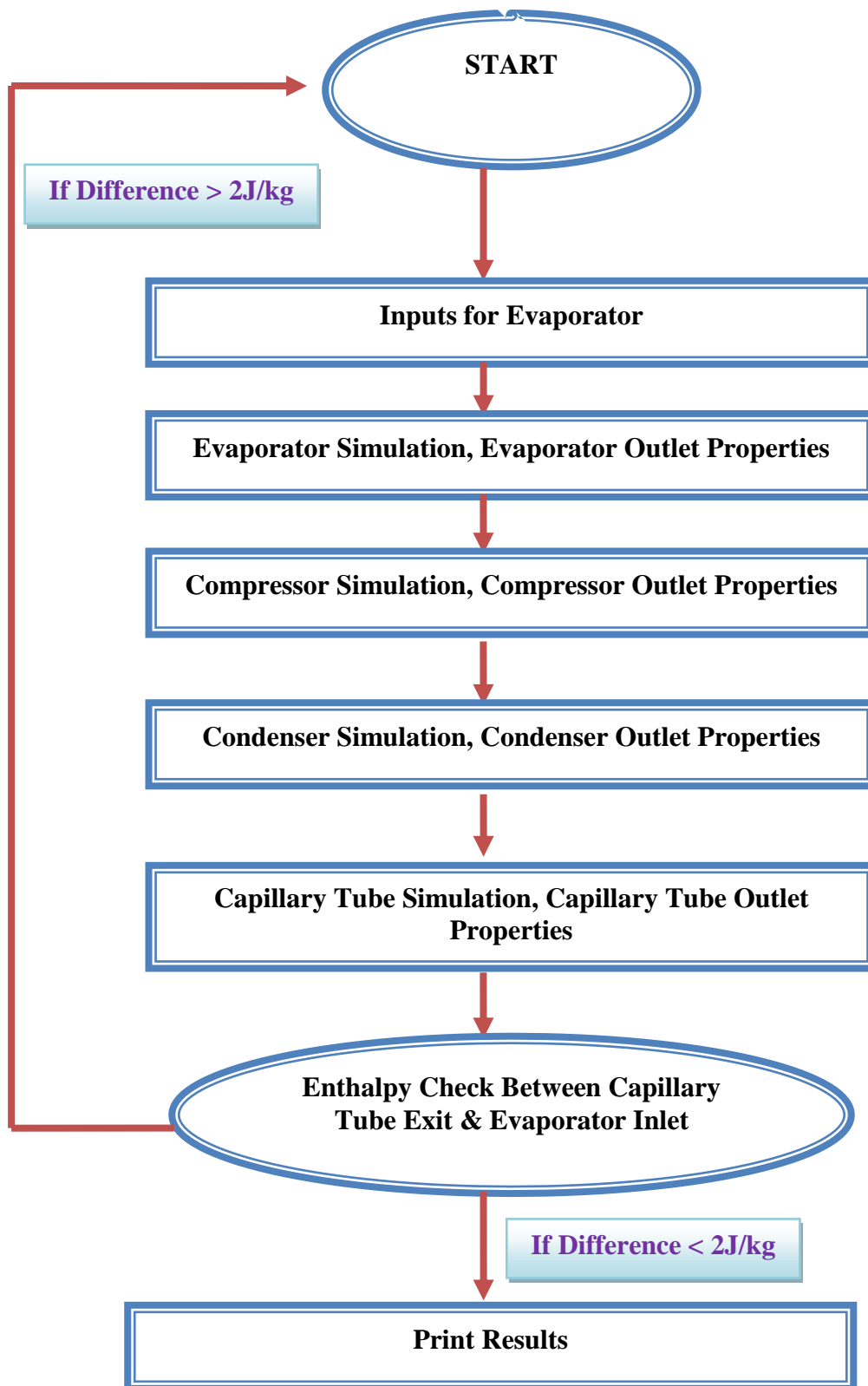


Figure 7. 1 Design Algorithm

### 7.3 Design and Simulation of a Micro VCRC

Actually, the design of a micro VCRC begins like that of a traditional VCRC. The heat load of the system should be determined first. After that, the evaporation and condensation temperatures should be decided. The operational conditions of the compressor and the capillary tube should be designated. In this study, an isentropic compressor and an isenthalpic capillary tube are selected. Knowing all these data and assuming an ideal cycle, an opinion about the mass flow rate of the refrigerant, the compressor pressure ratio, the condenser heat load and the COP of the system is formed. Designing each component one by one, and calculating the pressure drops in the condenser and the evaporator, a deviation from the ideal cycle line will occur. Therefore, a pre-determined state should be chosen and the design should be started from this state. Mostly, this is the inlet state of the evaporator. Since it is a cycle, the start and end points of the cycle should be nearly equal. Here, the starting state is the evaporator inlet and the end state is the capillary tube exit. The difference in the enthalpy values of these two states should not exceed 2 J/kg. If the desired value is not reached at the end of the design, calculations should be repeated with a new inlet enthalpy value of the evaporator as the mean value of capillary tube exit and the pre-determined evaporator enthalpy as

$$i_{evp_{new}} = \frac{i_{exp} + i_{evp}}{2}. \quad (7.1)$$

#### 7.3.1 Evaporator

An ideal cycle analysis yields a pre-determined state to begin the design of the evaporator. In the evaporator, there are two different regions with different flow regimes, which are the superheated vapor and two-phase mixture phases. Therefore, the design is performed separately in these two regions and the total length of the evaporator is calculated by summing the lengths in each of these regions.

### 7.3.1.1 Two Phase Mixture Regime

Steps in the algorithm used to solve the two phase regime problem in the evaporator may be listed as follows:

- Take the inlet state of the refrigerant as the fixed point from the ideal cycle analysis.
- Take the exit state temperature and pressure equal to the inlet state.
- Designate the vapor fraction of exit state as 1, which means saturated vapor.
- Define the required heat load.
- Calculate the mass flow rate.
- Assign a cold room temperature.
- Calculate the mean refrigerant temperature as:

$$T_{mean} = \frac{T_{inlet} + T_{exit}}{2} \quad (7.2)$$

- Read the inputs which are sorted as the

Channel height, channel width, channel thickness, number of the channels, and the base thickness.

- Designate a pre-determined segment length.
- Calculate all geometrical design parameters, which are the frontal area of the evaporator, the wetted perimeter, and the hydraulic diameter.
- Calculate the heat flux.
- Read material properties of the evaporator.
- Calculate the mass flux.
- Show the liquid phase based velocity of the refrigerant.
- Show the vapor phase based velocity of the refrigerant.
- Calculate the Reynolds number based on the liquid phase.
- Calculate the Reynolds number based on the vapor phase.

- Identify the Weber number based on the liquid phase.
- Determine the constant  $C$  according to the Reynolds number based on liquid and vapor phases.
- Calculate the rectangular aspect ratio.
- Define the Poiseuille number.
- Show the friction factor based on the liquid phase.
- Show the friction factor based on the vapor phase.
- Calculate the liquid phase frictional pressure drop per length.
- Calculate the vapor phase frictional pressure drop per length.
- Define the Martinelli parameter.
- Find the two phase multiplier.
- Show the two-phase frictional pressure drop of the refrigerant per unit length.
- Multiply the previous value with the segment length, which gives the total two phase frictional pressure drop of the refrigerant.
- Calculate the accelerational pressure drop.
- Sum up the frictional and accelerational pressure drops to get the total pressure drop.
- Subtract the total pressure drop from the inlet pressure of the refrigerant.
- Find the new saturation temperature of the vapor.
- Determine % error for the saturation temperature as:

$$error \% = \frac{T_{assumed} - T_{calculated}}{T_{assumed}} \times 100 \quad (7.3)$$

- If the % error value for the saturation temperature is less than 1%, continue calculation.
- Else if % error value for the saturation temperature is greater than 1%, assume a new exit temperature for the segment as:

$$T_{new} = \frac{T_{assumed} + T_{calculated}}{2} \quad (7.4)$$

- Calculate the boiling number.
- Calculate the convection number.
- Get the fluid surface parameter for R-134A.
- Calculate the heat transfer coefficient according to the Reynolds number based on the liquid phase and taking the liquid phase based Nusselt number as:
  - If  $Re_l < 100$ , calculate the two-phase flow heat transfer coefficient from (2.19).
  - Else if  $100 < Re_l < 1600$ , use (2.23) to calculate the liquid phase heat transfer coefficient.
  - Else if  $3000 < Re_l < 10^4$ , (2.24) may be used to find the liquid phase heat transfer coefficient.
  - Else if  $10^4 < Re_l < 5 \times 10^6$ , calculate the liquid phase heat transfer coefficient using (2.25).
  - If  $1600 < Re_l < 3000$ ,

$$h_{lo} = h_{l(Re_l=1600)} + \left( \frac{Re_l - 1600}{3000 - 1600} \right) (h_{l(Re_l=3000)} - h_{l(Re_l=1600)}) \quad (7.5)$$

- If  $Re_l > 100$ , two-phase heat transfer coefficient may be found from equations (2.20-22).
- Identify the tube surface temperature.
- Calculate the fin efficiency.
- Get the difference between the tube surface temperature and the film temperature.
- Find the real segment length.
- Calculate the % error in the segment length as:

$$\% \text{ error}_L = \frac{L_{real} - L_{assumed}}{L_{assumed}} \times 100. \quad (7.6)$$

- If the % error in the segment length is less than 1%, the calculation is completed successfully.
- Else if % error value of the segment length is greater than 1%, assume a new segment length as:

$$L_{new} = \frac{L_{assumed} + L_{real}}{2} \quad (7.7)$$

- Apply the procedure until the % error in the length is within 1%.

### 7.3.1.2 Single Phase Regime

Steps in the algorithm used to solve the single phase regime problem in the evaporator may be stated as follows:

- Take the inlet state as the exit state of the two-phase part.
- Define a temperature difference value for the superheated part.
- Take the exit temperature by subtracting the temperature difference from the inlet temperature under constant pressure.
- Assign a cold room temperature.
- Calculate the mean refrigerant temperature as:

$$T_{mean} = \frac{T_{inlet} + T_{exit}}{2} \quad (7.8)$$

- The read inputs may be listed as the mass flow rate, channel height, width and thickness, number of channels, base thickness.
- Designate a pre-determined segment length.

- Calculate all geometrical design parameters, which are the frontal area of the evaporator, the wetted perimeter, and the hydraulic diameter.
- Define the required heat load.
- Calculate the heat flux.
- Read material properties of the evaporator.
- Calculate the mass flux.
- Get the vapor mean velocity.
- Calculate the Reynolds number.
- Identify the friction coefficient.
- Determine the Nusselt number based on Gnielinski correlation.
- Read the constants  $D_o$  and  $C$ .
- Calculate the correction factor for Gnielinski correlation.
- Determine the new Nusselt number.
- Calculate the single phase heat transfer coefficient.
- Show the pressure drop value.
- Identify the tube surface temperature.
- Calculate the fin efficiency.
- Obtain the difference between the tube surface temperature and the film temperature.
- Find the real segment length.
- Calculate the % error in the segment length as

$$\% error_L = \frac{L_{real} - L_{assumed}}{L_{assumed}} \times 100. \quad (7.9)$$

- If the % error in the segment length is smaller than 1%, the calculation are completed successfully.
- Else if the % error value in the segment length is greater than 1%, a new segment length is assumed:

$$L_{new} = \frac{L_{assumed} + L_{real}}{2} \quad (7.10)$$

- Apply the procedure until the % error in the length stays within 1%.

### **7.3.2 Compressor Design**

The compressor design begins at the exit state of the evaporator. The properties of this state are known. Since the condensation pressure is known, the pressure ratio of the compressor is known at the beginning. It should be known that designing a compressor is to design its principle dimensions which may be listed as the

Stroke, bore diameter, suction and discharge valve pressure fractions and leakage fraction, clearance factor, number of cylinders

Since the system is a microscale VCRC, the number of the cylinders is selected as unity. The stroke and the bore diameters are decided first. An isentropic compressor is considered in the design. Power requirement of the compressor is found. Moreover, the volumetric and clearance efficiencies, the swept and suction volumes and the piston speed are calculated.

Steps in the compressor design:

- Take the inlet state as the exit state of the evaporator.
- Take the entropy of exit state equal to inlet entropy.
- Designate the exit state.
- Read the thermophysical properties of the refrigerant at the inlet and exit states.
- Read inputs which may be listed as the mass flow rate, stroke, stroke/bore diameter ratio, suction valve pressure fraction, discharge valve pressure fraction, the leakage fraction, the clearance factor, and the number of cylinders.
- Pre-determine the rotational speed of the compressor.
- Calculate the bore diameter.

- Determine the swept volume.
- Calculate the suction pressure.
- Calculate the discharge pressure.
- Calculate the specific work of the compressor.
- Calculate the compressor power requirement.
- Determine the volumetric efficiency.
- Determine the clearance volume.
- Determine the suction volume.
- Calculate the rotational speed and the mean velocity of the compressor.
- Find the % error between the calculated and the assumed values for the rotational speed as:

$$error \% = \frac{N_{calculated} - N_{assumed}}{N_{assumed}} \times 100 \quad (7.11)$$

- If the % error is less than 1%, the design is completed.
- Else, assume new stroke.
- Repeat the procedure until the % error in the rotational speed stays under 1%.

### 7.3.3 Condenser Design

In the condenser design, the principle dimensions of the condenser are determined both the in refrigerant side and the air side. The principle dimensions of a condenser may be given as the tube height, tube depth, the number of channels, the diameter of the channels, the length of the tube, the fin pitch, length and thickness, the louver angle, pitch and length.

Since inside the condenser tubes there are two different flow regimes, namely, the superheated vapor and the two-phase mixture, the lengths of these regions are calculated separately, and sum of these lengths gives the total length of the

condenser. The superheated vapor, which leaves the compressor, enters the condenser and leaves as a saturated liquid. The algorithm steps for the condenser are presented next.

### **7.3.3.1 Superheated Vapor Regime**

The algorithm steps for the superheated refrigerant side and the airside of the condenser may be summarized as follows:

For Refrigerant Side:

- Take inlet state as the exit state of the compressor.
- State the thermophysical properties at the inlet state.
- Obtain the condensation temperature taking the pressure of inlet state as constant.
- Determine the thermophysical properties at the exit state.
- Read inputs which may be listed as the mass flow rate, the segment length, the channel height and depth, the number of channels, the diameter of channels, the fin pitch, length and thickness, the louver angle, pitch and length.
- Calculate all geometrical design parameters, which are the frontal area of the condenser, the wetted perimeter and the hydraulic diameter.
- Determine the Reynolds number.
- Determine the friction coefficient.
- Determine the Nusselt number based on the Reynolds number.
- Calculate the heat transfer coefficient.
- Calculate the refrigerant side total pressure drop.
- Subtract the inner side pressure drop value from the inlet pressure value of the refrigerant.
- Find the condensation temperature of the refrigerant at this pressure.
- Calculate the error between the assumed and calculated values of the condensation temperature of refrigerant as:

$$error \% = \frac{T_{calculated} - T_{assumed}}{T_{assumed}} \times 100 \quad (7.12)$$

- If the % error in the condensation temperature is less than 1%, continue.
- Else, assume new condensation temperature as:

$$T_{cond.} = \frac{T_{calculated} + T_{predetermined}}{2} \quad (7.13)$$

For Airflow Side:

- Define a room temperature.
- Take the room temperature as the air inlet temperature.
- Determine a differential temperature between the air inlet and exit temperatures.
- Add the differential to the air inlet temperature, which gives the air exit temperature.
- State the thermophysical properties of the air at the average of air inlet and exit temperatures.
- Calculate all geometrical design parameters, such as, the free flow area, the wetted perimeter and the hydraulic diameter of the air, the total fin area, and the total outer area.
- Calculate the air side Reynolds number based on the louver pitch.
- Determine the mean air velocity.
- Obtain the Colburn-j factor.
- Define the air side friction factor.
- Provide the power required for air supply.
- Determine the air side fin efficiency.
- Calculate the overall fin efficiency.
- Determine the air side pressure drop value.

For the Overall System:

- Calculate the overall heat transfer coefficient.
- Determine the minimum heat capacitance.
- Determine the number of transfer units.
- Find the maximum heat transfer.
- Determine the effectiveness.
- Identify the total heat transfer ratio.
- Calculate air exit temperature.
- Designate the % error between the assumed and calculated values of the air exit temperature as:

$$error \% = \frac{T_{calculated} - T_{assumed}}{T_{assumed}} \times 100 \quad (7.14)$$

- If the % error is less than 1%, calculations are completed successfully.
- Else, assume a new air exit temperature, and apply the procedure again.

### 7.3.3.2 Two Phase Mixture Condensation Regime

For the refrigerant side:

- Take the inlet state as saturated vapor leaving the superheated region of the condenser.
- State thermophysical properties at the inlet.
- Read inputs which are the mass flow rate, the channel height, the channel depth, the number of the channels, the diameter of the channels, fin pitch, length and thickness, louver angle, pitch and length.
- Designate a pre-determined segment length.
- Calculate all geometrical design parameters, which are the frontal area of the condenser, the wetted perimeter and the hydraulic diameter.
- Assume a vapor fraction at the exit of the segment under constant pressure and temperature.

- Take the average of inlet and exit state vapor fractions.
- Evaluate the refrigerant properties at the average vapor fraction value.
- Calculate the mass flux.
- Calculate the velocity of the liquid phase.
- Calculate the velocity of the vapor phase.
- Determine the void fraction value.
- Determine the liquid phase based on the Reynolds number.
- Determine the vapor phase based on Reynolds number.
- Calculate the liquid super-facial velocity.
- Calculate the surface tension parameter.
- Calculate the Martinelli parameter.
- If the liquid phase based Reynolds number is less than 2100  
Assign the variables as follows as in equation (4.21).
- Else if the liquid phase based Reynolds number is greater than 2100.  
Assign the variables as follows as in equation (4.22).
- Calculate the interfacial friction factor.
- Determine the refrigerant side pressure drop.
- Determine the interfacial shear stress.
- Obtain the dimensionless friction velocity.
- Determine the turbulent film thickness.
- Identify the dimensionless turbulent film thickness.
- Identify the turbulent dimensionless temperature in terms of the liquid phase based Reynolds number.
- Identify the turbulent dimensionless temperature.
- Determine the refrigerant side heat transfer coefficient.

For the airflow side:

- Define a room temperature.
- Take the room temperature as the air inlet temperature.
- Determine a differential between air inlet and exit temperature.

- Add the differential to air inlet temperature, which gives air exit temperature.
- State the thermophysical properties of the air at the average value of the air inlet and exit temperatures.
- Calculate all geometrical design parameters, which are given as:

Free flow area, the wetted perimeter and hydraulic diameter of air, the total fin area, the total outer area.

- Calculate air side Reynolds number based on the louver pitch.
- Determine the mean air velocity.
- Get the Colburn-*j* factor.
- Define the air side friction factor.
- Provide the power required for the air supply.
- Read the material properties of the condenser.
- Determine the air side fin efficiency.
- Calculate the overall fin efficiency.
- Determine the air side pressure drop.

For the overall system:

- Calculate the overall heat transfer coefficient.
- Determine the minimum heat capacitance.
- Determine the number of transfer units.
- Find maximum heat transfer.
- Obtain the effectiveness.
- Identify the total heat transfer ratio.
- Calculate the enthalpy of the refrigerant at the exit of the segment.
- Determine refrigerant exit vapor fraction value.
- Show the % error value for the enthalpy as:

$$error \% = \frac{i_{calculated} - i_{assumed}}{i_{assumed}} \times 100 \quad (7.15)$$

- If the % error value of enthalpy smaller than 1%, continue calculation.
- Else, assume a new vapor fraction value for the exit state of the segment as:

$$x_{new} = (x_{calculated} + x_{assumed})/2 \quad (7.16)$$

- Subtract the refrigerant side pressure drop value from the inlet pressure of the refrigerant.
- Find the new condensation temperature.
- Determine the % error in the condensation temperature as:

$$error \% = \frac{T_{assumed} - T_{calculated}}{T_{assumed}} \times 100 \quad (7.17)$$

- If the % error is less than 1%, proceed.
- Else, assume a new exit temperature for the segment.
- Calculate the air side exit temperature.
- Find the % error between the assumed and the calculated temperature values of air side as:

$$error \% = \frac{T_{assumed} - T_{calculated}}{T_{assumed}} \times 100 \quad (7.18)$$

- If % error value of air side exit temperature is less than 1%, then stop calculations.
- Else, assume a new air side exit temperature.
- Take the newly calculated vapor fraction, temperature and pressure values as the inlet state of the second segment.
- Apply the procedure again for every segment until the vapor fraction reaches the value of 0 with an error less than 1%.

### 7.3.4 Capillary Tube

Design algorithm for the sizing of the capillary tube is given as follows:

- Take the inlet state of the refrigerant as the exit state of the condenser.
- Read the evaporator temperature and pressure as inputs.
- Choose a diameter value for the tube.
- Determine the temperature difference between the inlet and exit states.
- Divide the tube into a selected number of segments with equal temperature differences.
- Read the inlet and exit saturation properties.
- Take the exit enthalpy being equal to the inlet enthalpy.
- Find the exit vapor fraction.
- Evaluate the inlet and exit state properties using the vapor fractions.
- Evaluate the thermophysical properties of the refrigerant as the mean values of inlet and exit states.
- Find the inlet velocity.
- Find the exit velocity.
- Take the tube velocity as the mean value.
- If the exit velocity is greater than the sound velocity, stop calculations and select a tube with a greater diameter.
- Identify the Reynolds number.
- If the Reynolds number is less than 2300 calculate the friction factor from (5.10).
- Else, use (5.11) to find the friction factor.
- Calculate the length of the segment.
- Take the exit state of the first segment as the inlet state of the second segment.
- Apply the procedure until the last segment length is found.
- Total length of the hose is the sum of the lengths of all segments.

- If the total length of the hose becomes greater than 2 meters, select a tube with a smaller hydraulic diameter and repeat all calculations.

## **CHAPTER 8**

### **RESULTS**

#### **8.1 General**

The micro-scale VCRC has been designed and analyzed first with an isentropic compressor, then with a polytropic one. For both cases, two alternative designs for the evaporator as suggested in Chapter 2 are considered.

Throughout the design and analyses, the cold room temperature is selected to be 15°C and the ambient temperature is selected as 30°C.

The results for each component and the complete cycle with the isentropic compressor are presented in Section 8.2 and those with the polytropic compressor are stated in Section 8.3.

#### **8.2 Results of Micro VCRC with Isentropic Compressor**

The results for the original evaporator, with rectangular microchannels, are given in Table 8.1. The total pressure drop in the evaporator is nearly 5080 Pa. 4600 Pa of this loss occurs in the two phase region and only 480 Pa in the single phase region. Accelerational pressure drop in the two phase region is about 1345 Pa and the frictional pressure drop is 3255 Pa. In the two phase region, the liquid phase based Reynolds number is 87 and the vapor phase based Reynolds number is

4836. In the single phase region, the Reynolds number is 6840. The liquid velocity is about 0.0433 m/s and vapor velocity is about 8.25 m/s. The single phase velocity is about 12.9 m/s. The two phase region heat transfer coefficient is 19030 W/m<sup>2</sup>K while the single phase region heat transfer coefficient is 966 W/m<sup>2</sup>K.

**Table 8. 1** Evaporator Results

<b>Cold Room Temperature (°C)</b>	15		<i>Inlet State</i>	<i>Exit State</i>
<b>Length of Two-Phase Region (mm)</b>	13	<b>Temperature (°C)</b>	0	3
<b>Length of Superheated Region (mm)</b>	5.4	<b>Pressure (MPa)</b>	0.29269	0.28761
<b>Total Length of Evaporator (mm)</b>	18.4	<b>Enthalpy (kJ/kg)</b>	271.59	401.3
<b>Channel Height (mm)</b>	0.4	<b>Entropy (kJ/kgK)</b>	1.2621	1.738
<b>Channel Width (mm)</b>	0.5	<b>Evaporator Capacity (W)</b>	45	
<b>Number of Channels</b>	10			

**Table 8. 2** Alternative Evaporator Results

<b>Cold Room Temperature (°C)</b>	15		<i>Inlet State</i>	<i>Exit State</i>
<b>Length of Two-Phase Region (mm)</b>	10	<b>Temperature (°C)</b>	0	3
<b>Length of Superheated Region (mm)</b>	4.4	<b>Pressure (MPa)</b>	0.29269	0.28761
<b>Channel Diameter (mm)</b>	0.52	<b>Enthalpy (kJ/kg)</b>	271.59	401.3
<b>Number of Channels</b>	8	<b>Entropy (kJ/kgK)</b>	1.2621	1.738
<b>Base Thickness (mm)</b>	1	<b>Evaporator Capacity (W)</b>	45	
<b>Total Length of Evaporator (mm)</b>	14.4			

Results for the alternative evaporator, with circular tubes, are given in Table 8.2. The total pressure drop in the alternative evaporator is nearly 5080 Pa where 4640 Pa is in the two phase region and 440 Pa is in single phase region. Accelerational pressure drop in the two phase region is about 1826 Pa. and the frictional pressure drop is 2814 Pa. In two phase region, the liquid phase based Reynolds number is 119 and vapor phase based Reynolds number is 6660, while the single phase Reynolds number is 9422. The liquid velocity is about 0.0509 m/s and the vapor velocity is about 9.72 m/s. The single phase velocity is about 15.2 m/s. Two phase region heat transfer coefficient is 25220 W/m<sup>2</sup>K while single phase region heat transfer coefficient is 1177 W/m<sup>2</sup>K.

Compressor results are summarized in Table 8.3.

**Table 8. 3** Compressor Results

Number of Cylinders	1	Clearance Efficiency (%)	85.02		<i>Inlet State</i>	<i>Exit State</i>
Pressure Fraction Through Suction Valve	0.95	Overall Volumetric Efficiency (%)	75.31	Temperature (°C)	3	58.05
Pressure Fraction Through Discharge Valve	0.95	Compressor Power (W)	11.1	Pressure (MPa)	0.28761	1.3177
Clearance Factor	0.05	Compressor Speed (rpm)	500	Enthalpy (kJ/kg)	401.3	433.13
Stroke (mm)	51.8			Entropy (kJ/kgK)	1.738	1.738
Bore Diameter (mm)	10.4					
Isentropic Index	1.136					

**Table 8. 4** Condenser Results

<b>Room Temperature (°C)</b>	30	<b>Refrigerant Side</b>	<i>Inlet State</i>	<i>Exit State</i>
<b>Condenser Capacity (W)</b>	56.8	Temperature (°C)	58.05	49.95
<b>Superheated Region Length (mm)</b>	14	Pressure (MPa)	1.3177	1.3160
<b>Two-Phase Region Length (mm)</b>	170	Enthalpy (kJ/kg)	433.13	271.51
<b>Total Condenser Length (mm)</b>	184	Entropy (kJ/kgK)	1.738	1.2371
<b>Fin Efficiency (%)</b>	77.95	<b>Air Side</b>	<i>Inlet State</i>	<i>Exit State</i>
<b>Fan Power (W)</b>	0.3	Temperature (°C)	30	37

Condenser results are presented in Table 8.4. The total pressure drop in the condenser is nearly 1903 Pa where 1653 Pa is in the two phase region and 250 Pa in the single phase region. In two phase region, the condensation heat transfer coefficient is plotted against the condenser length in Figure 8.1. Plots for the air side, the refrigerant side and the overall heat transfer coefficients with respect to the length are given in Figure 8.2. The liquid phase based Reynolds number, and the vapor phase based Reynolds number are also plotted with respect to the length as shown in Figure 8.3. The single phase Reynolds number is 6394, and the corresponding velocity is 2.78 m/s. The heat transfer coefficient is 1164 W/m<sup>2</sup>K and the overall heat transfer coefficient in the single phase region is

about 42.5 W/m<sup>2</sup>K. The air side velocity is calculated as 4.376 m/s along the flow direction.

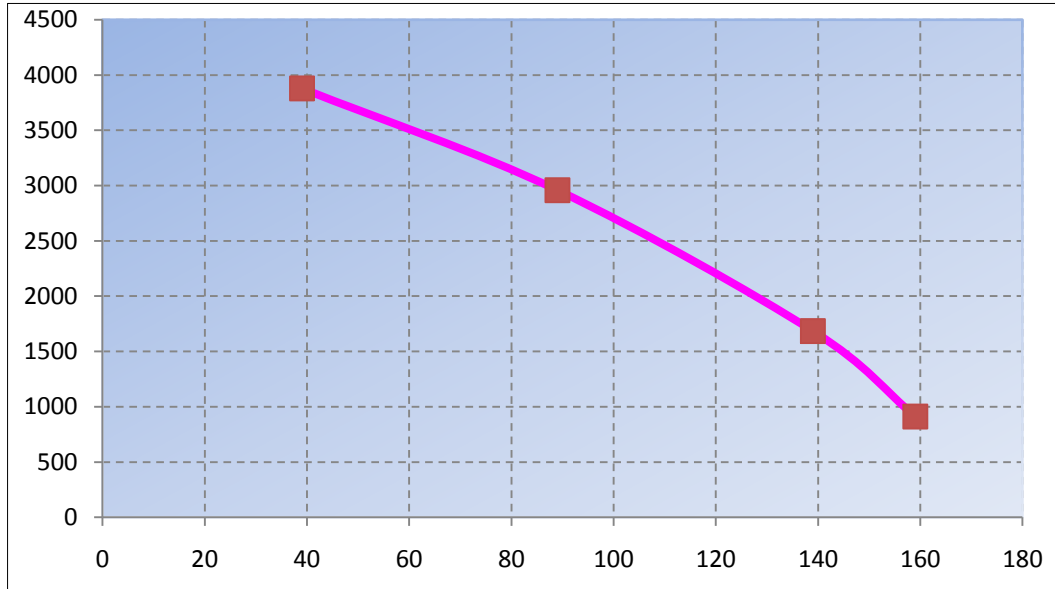


**Figure 8. 1** Condensation Heat Transfer Coefficient (W/m<sup>2</sup>K) vs. Length (mm)

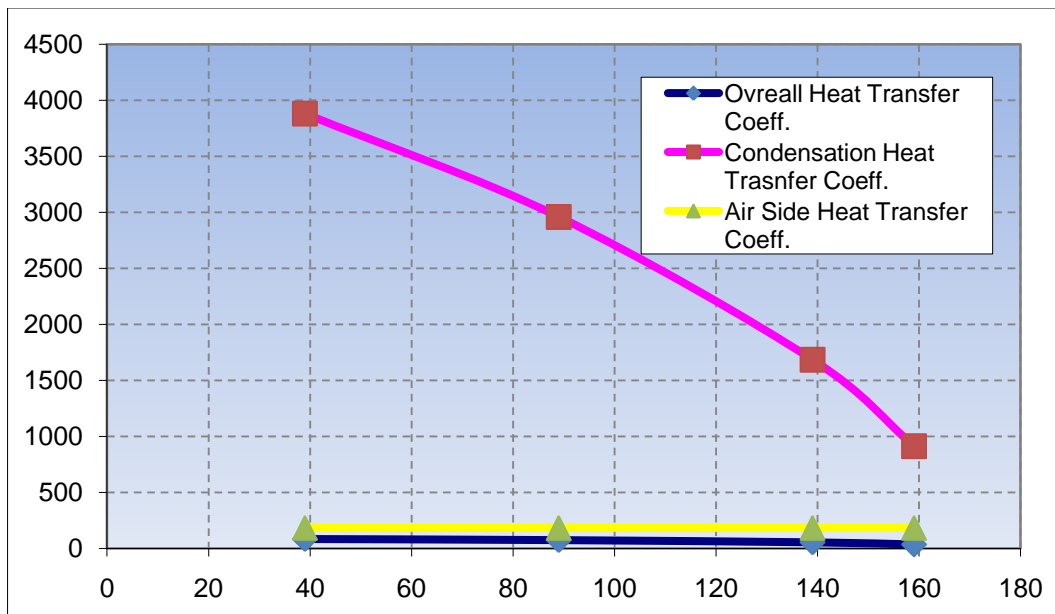


**Figure 8. 2** Heat Transfer Coefficients (W/m<sup>2</sup>K) vs. Length (mm)

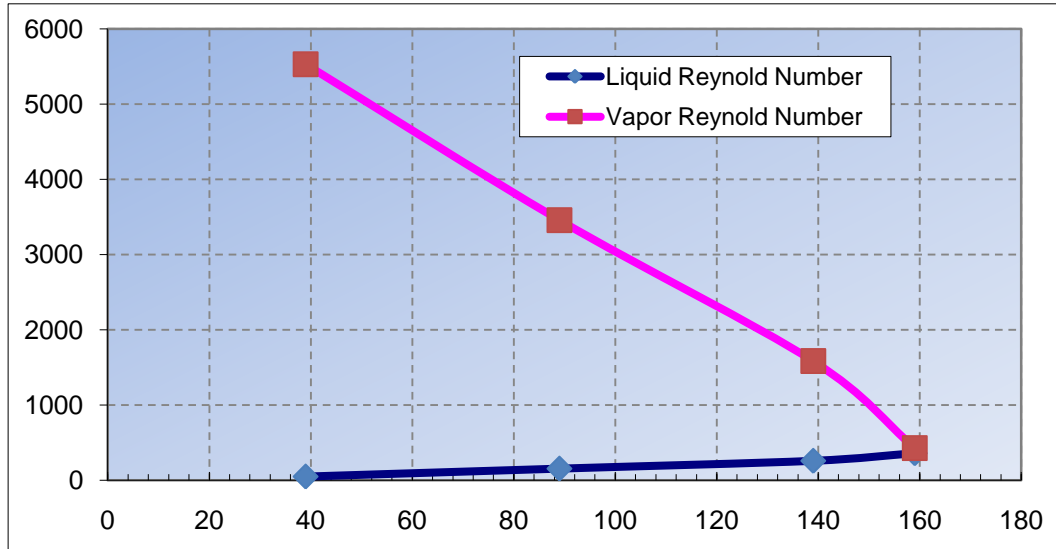


**Figure 8. 3** Reynolds Number vs. Length (mm)

**Table 8. 5** Capillary Tube Design

<b>Diameter (mm)</b>	0.4		
<b>Length (m)</b>	0.721		
		<i>Inlet State</i>	<i>Exit State</i>
	<b>Temperature (°C)</b>	49.95	0
	<b>Pressure (MPa)</b>	1.3160	0.29269
	<b>Enthalpy (kJ/kg)</b>	271.51	271.59
	<b>Entropy (kJ/kgK)</b>	1.2371	1.2621

**Table 8. 6** Cycle Parameters

<b>Mass Flow Rate of Refrigerant (g/s)</b>	0.35	<b>Maximum Temperature (°C)</b>	58.05
<b>Coefficient of Performance</b>	3.89	<b>Maximum Pressure (MPa)</b>	1.3177
<b>Evaporator Saturation Temperature (°C)</b>	0	<b>Total Irreversibility (W)</b>	9.2275
<b>Condenser Saturation Temperature (°C)</b>	50		

Capillary tube results and the cycle analysis data are given in Tables 8.5 and 8.6, respectively. The temperature vs. entropy and pressure vs. enthalpy diagrams of the vapor compression cycle with an isentropic compressor are given in Figures 8.4 and 8.5, respectively.

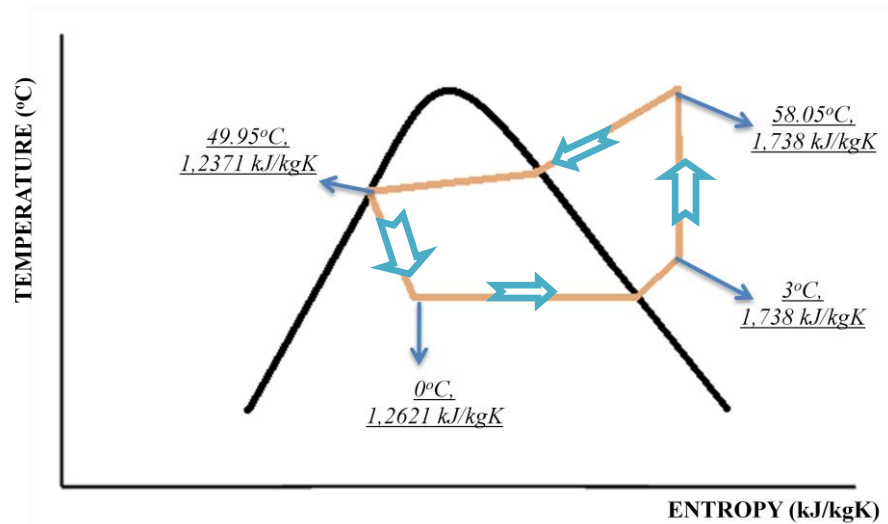


**Figure 8. 4** Temperature vs. Entropy with Isentropic Compressor

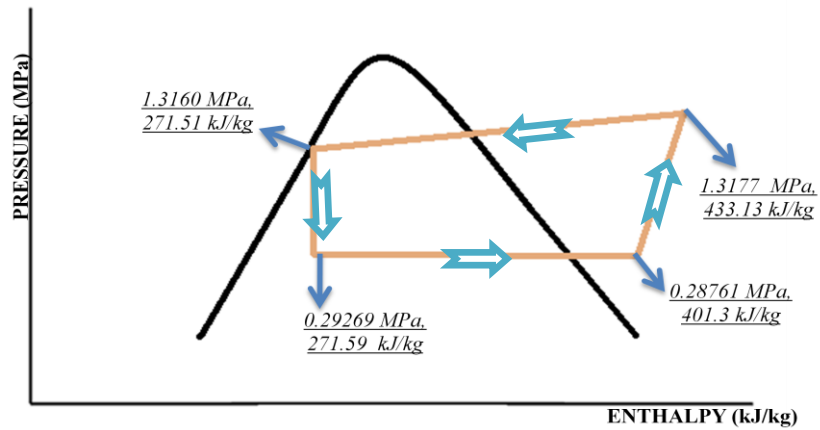


**Figure 8. 5** Pressure vs. Enthalpy with Isentropic Compressor

### 8.3 Results of Micro VCRC with Polytropic Compressor

Evaporator, alternative evaporator, polytropic compressor, condenser, capillary tube results and the cycle data for the vapor compression refrigeration cycle with a polytropic compressor are presented in Tables 8.7-12.

**Table 8. 7** Evaporator Results

Cold Room Temperature (°C)	15		<i>Inlet State</i>	<i>Exit State</i>
Length of Two-Phase Region (mm)	13	Temperature (°C)	0	3
Length of Superheated Region (mm)	5.4	Pressure (MPa)	0.29269	0.28761
Channel Height (mm)	0.4	Enthalpy (kJ/kg)	271.59	401.3
Channel Width (mm)	0.5	Entropy (kJ/kgK)	1.2621	1.738
Number of Channels	10	Evaporator Capacity (W)	45	
Total Length of Evaporator (mm)	18.4			

**Table 8. 8** Alternative Evaporator Results

Cold Room Temperature (°C)	15		<i>Inlet State</i>	<i>Exit State</i>
Length of Two-Phase Region (mm)	10	Temperature (°C)	0	3
Length of Superheated Region (mm)	4.4	Pressure (MPa)	0.29269	0.28761
Channel Diameter (mm)	0.52	Enthalpy (kJ/kg)	271.59	401.3
Number of Channels	8	Entropy (kJ/kgK)	1.2621	1.738
Base Thickness (mm)	1	Evaporator Capacity (W)	45	
Total Length of Evaporator (mm)	14.4			

It should be noted that the inlet and exit states of the two evaporators are kept the same both for the isentropic and polytropic compressors.

**Table 8. 9** Compressor Results

Number of Cylinders	1	Clearance Efficiency (%)	86.45		<i>Inlet State</i>	<i>Exit State</i>
Pressure Fraction Through Suction Valve	0.95	Overall Volumetric Efficiency (%)	76.98	Temperature (°C)	3	82.7
Pressure Fraction Through Discharge Valve	0.95	Compressor Power (W)	20.81	Pressure (MPa)	0.28761	1.3177
Clearance Factor	0.05	Compressor Speed (rpm)	500	Enthalpy (kJ/kg)	401.3	460.76
Stroke (mm)	51.4			Entropy (kJ/kgK)	1.738	1.8172
Bore Diameter (mm)	10.3					
Polytropic Index	1.2					

**Table 8. 10** Condenser Results

Room Temperature (°C)	30	<b>Refrigerant Side:</b>	<i>Inlet State</i>	<i>Exit State</i>
Condenser Capacity (W)	56.8	Temperature (°C)	82.7	49.93
Superheated Region Length	43	Pressure (MPa)	1.3177	1.3154
Two-Phase Region Length	170	Enthalpy (kJ/kg)	460.76	271.51
Total Condenser Length (mm)	213	Entropy (kJ/kgK)	1.8172	1.2371
Fin Efficiency	77.95	<b>Air Side:</b>	<i>Inlet State</i>	<i>Exit State</i>
Fan Power (W)	0.346	Temperature (°C)	30	37.5

For the polytropic compressor, only in the single phase region of the condenser, different results are obtained compared to those obtained with an isentropic compressor. The single phase pressure drop is obtained as 852 Pa, the Reynolds number is 5806, the velocity is 3.02 m/s, the heat transfer coefficient is 1232 W/m<sup>2</sup>K and the overall heat transfer coefficient in single phase region is about 44.24 W/m<sup>2</sup>K.

**Table 8. 11** Capillary Tube Design

Diameter (mm)	0.4		
Length (m)	0.721		
		<i>Inlet State</i>	<i>Exit State</i>
	Temperature (°C)	49.93	0
	Pressure (MPa)	1.3160	0.29269
	Enthalpy (kJ/kg)	271.51	271.59
	Entropy (kJ/kgK)	1.2371	1.2621

**Table 8. 12** Cycle Parameters

Mass Flow Rate of Refrigerant (g/s)	0.35	Maximum Temperature (°C)	86.2
Coefficient of Performance	2.12	Maximum Pressure (MPa)	1.3177
Evaporator Saturation Temperature (°C)	0	Total Irreversibility (W)	18.8975
Condenser Saturation Temperature (°C)	50		

It is shown that the polytropic compression needs more work in the cycle. The total irreversibility is also higher in the polytropic compression case. The same capillary tube and the evaporator are used as those in the isentropic compression cycle. Temperature vs. entropy and pressure vs. enthalpy diagrams of the polytropic cycle are given in Figures 8.6 and 8.7.

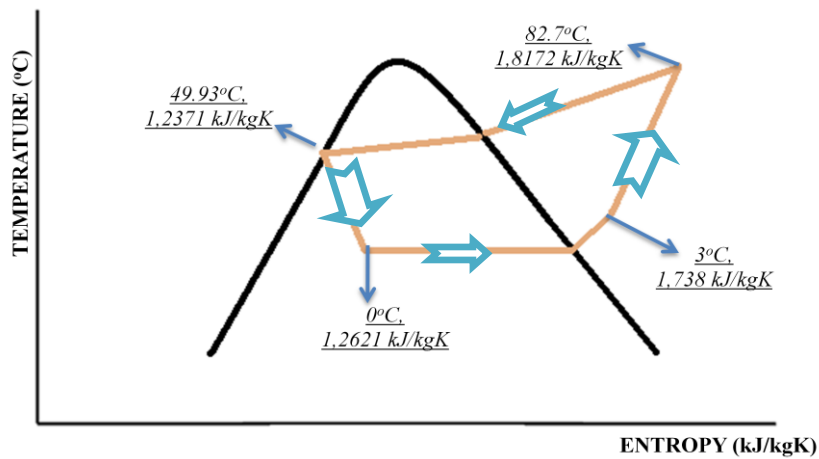


**Figure 8. 6** Temperature vs. Entropy with Polytropic Compressor

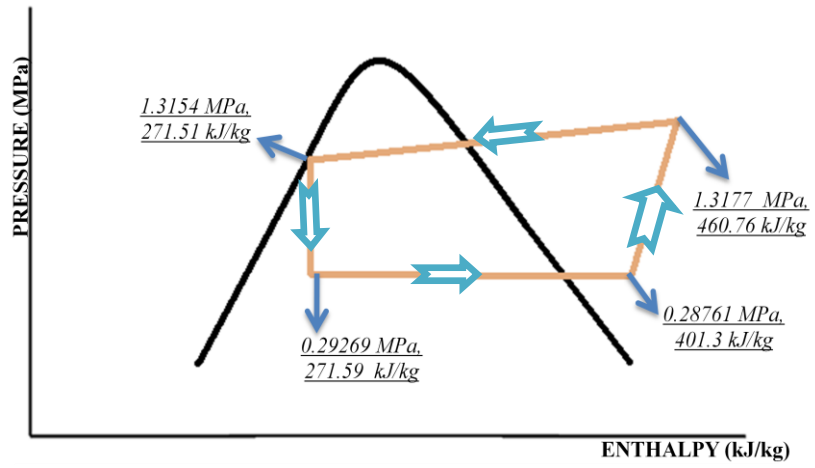


**Figure 8. 7** Pressure vs. Enthalpy with Polytropic Compressor

## CHAPTER 9

### DISCUSSION AND CONCLUSION

#### 9.1 Discussion and Conclusion

In this study, a vapor compression refrigeration cycle is designed for a micro refrigerator. Firstly, the reason for the use of the word “micro” in the name of the study is explained. Apparently, the categorization of the channels changes from author to author. The condenser and the evaporator designed in this study may be classified as microchannels based on the studies of Serizawa [3], and Kew and Cornwell [4]. After that, the related studies in the literature are discussed. Then, a cycle analysis is performed and all four components of a micro refrigerator are designed one by one.

The results are presented in Chapter 8. First, the evaporator is designed. After determining heat load and evaporation temperature, the dimensions of the evaporator are set. The main point in the evaporator design is that the heat transfer coefficient in the two phase region is really high compared to any conventional channel evaporation. This shows the beauty of the use of microchannels. On the other hand, the single phase flow heat transfer coefficient is found to be about 1/19 of that of the two phase region. For this reason, although the length of the single phase region is nearly equals the half of the two phase region length, the heat transfer rate in single phase region is very small compared to that in the two phase region.

Moreover, attention should be paid to the pressure drops. The pressure drop in the two phase region is due to the friction and acceleration. However, since the mass flow rate is small, the pressure drop is not so high. Only 0.45°C difference occurs between the inlet and the exit states of the two phase region. In the single phase region, the pressure drop is due to friction only and its value is about 1/10 of that in the two phase region. Another important characteristic of the two phase flow in microchannels is that the liquid based Reynolds number is always in the laminar flow region whereas the vapor based Reynolds number falls nearly always in the turbulent regime.

Another important point of this study is the design of an alternative evaporator for the cycle. The alternative evaporator has circular tubes while the original evaporator had rectangular channels. The design criterion for the alternative evaporator is to work between same states and to get nearly same pressure drop as the original evaporator. It is seen that the heat transfer coefficient in the alternative evaporator is higher than the original one in both single phase and two phase regions. Therefore, the length of that evaporator is selected shorter than the original one. It has been concluded that both evaporators can be used in the cycle and selection must be made based on the manufacturing considerations as well as the space limitations.

The heat transfer rate to volume ratio of the original and alternative evaporators are found to be about 1.67 W/cm<sup>3</sup> and 2.05 W/cm<sup>3</sup>, respectively. These ratios show the high compactness of the evaporators.

After designing the evaporator, the compressor design is performed. An isentropic compressor is used first. For the purpose of COP comparison, a polytropic compressor is designed and analyzed as well. The speed of the compressor is selected as 500 rpm and the principle dimensions are determined. The stroke over diameter ratio is selected as 5 at the beginning of the design. The length of the compressor may seem very short and it may be thought that it is

hard to find such a small motor for the compressor. However, with the advances in the manufacturing technology, such compressors and motors are believed to be buildable today. Besides, since microscale and pressure sensitive opening and closing valves are used as the suction and discharge valves, the mechanical losses may be diminished considerably.

Since all compressors must work with an index of compression between isentropic ( $n = k$ ) and isochoric ( $n = \infty$ ), a polytropic index of 1.2 is selected to compare the results with those for an isentropic compressor. Obviously, the temperature at the exit state is higher for a polytropic compressor than the isentropic one, which leads to a higher heat transfer rate from the condenser when the saturation temperatures are held constant. Since the condenser heat load becomes higher and the evaporator heat load is constant, a smaller COP value is obtained with polytropic compression process.

Condenser design was the most difficult part of the study due to the lack of studies on micro-scale condensers and their geometric details. The refrigerant side flow has two portions, the single phase flow and the two phase flow. Like in the evaporator, the two phase flow heat transfer coefficient is very high in microchannels compared to conventional channels. The single phase heat transfer coefficient is also high too but its value is very small compared to that of the two phase region. The Reynolds number based on the liquid phase is always in the laminar region whereas the vapor phase based Reynolds number is in the turbulent region. An important point here is that since the air side heat transfer coefficient is much smaller than the refrigerant side, the dominant part in the overall heat transfer coefficient is due to the air side heat transfer.

The air side geometry of the condenser is selected with a high attention. Since forced convection is preferred on the air side, the fin design plays an important role. The influence of the louvered fin geometry on the flow and heat transfer should be investigated carefully. Moreover, the air side velocity should be kept

under a reasonable value. For the condenser design, the room temperature is selected as 30°C.

The last equipment to be designed was the capillary tube. Two phase flow occurs in the capillary tube and its role on the pressure drop cannot be denied. Since the temperature, pressure and vapor fraction change along the length of the capillary tube, it is an obligation to use finite segments in its design calculations. It should be known that the length of a capillary tube is highly dependent on the diameter of the tube. For example, a tube with a diameter of 0.5 mm should be 2.16 m long, whereas with a tube diameter of 0.4 mm, a length of 0.72 m is sufficient to work between the same states.

After designing all four components in the cycle, a second law analysis is performed for the cycle. The second law analysis in the refrigeration cycle depends on the irreversibility of the cycle which is due to entropy generation in the components. The difference between the polytropic and isentropic compression processes are observed in this study.

The cycle is checked against a possible condensation problem that may occur if it is placed in contact with an electrical device due to the low evaporation and cold room temperatures. However, for the winter season, the dew point is calculated below 10°C and for the summer season below 15°C, respectively. Therefore, no condensation problem is expected on the walls of the evaporator for this cycle.

During the construction of the cycle, the most important issue is to insulate the compressor, capillary tube, the sides of the evaporator and all the connection pipes very carefully to prevent the heat transfer between the equipments and the surroundings.

To decide where to put the present study in the literature and to compare the results, Table 9.1 may help.

**Table 9. 1** Comparison of present study with literature

	<b>Chow et al. [20]</b>	<b>Heydari [21]</b>	<b>Phelan et al. [22]</b>	<b>Chriac and Chriac [23]</b>	<b>Mongia [24]</b>	<b>Present Study</b>
<b>Heat Load (W)</b>	32	-	100-300	100	50	45
<b>T evp. (°C)</b>	12	20	5	10	50	0
<b>Tcond. (°C)</b> <b>{Tamb. (°C)}</b>	- {45}	60 -	55 -	55 -	90 {50}	50 {30}
<b>Flow Rate (g/s)</b>	16.3		0.824 - 2.47	12.5 <sub>3</sub> (cm <sup>3</sup> /s)	0.26	0.35
<b>System Volume</b>	Meso-scale	CPU Cooling System	Meso Scale	-	Notebook Cooling	Micro Scale
<b>Refrigerant</b>	R-134A	R-134A	R-134A	R-134A	R-600A	R-134A
<b>COP</b>	3.34	3.0	3	4.5	2.25	3.89
<b>Compressor Type</b>	Centrifugal	Piston	Scroll	Scroll	-	Piston

It is seen that the study of Mongia [24] may be compared with the present study in terms of the sizes of the cycle. However, it should be noted that the study of Mongia [24] is an experimental study. Therefore, the present study may be thought as a milestone in the literature where a micro-scale refrigerator with all of the components is designed theoretically.

In conclusion, a micro refrigerator has been successfully designed and analyzed within the scope of this thesis. The results actually indicate that it is possible to construct and test such a cycle.

## 9.2 Future Work

For different application areas, the cycle may be analyzed for different temperatures, pressures and for different refrigerants. Moreover, an optimization

study on the components may be performed. Different types of compressors may be designed for the cycle, such as, screw, centrifugal or scroll compressors.

In the present study, a steady-state analysis of the refrigeration cycle has been performed. The transient response of the cycle may also be investigated. The effect of radiation in the condenser and the evaporator may be taken into account during the design.

The designed cycle would be constructed and tested during the operation to verify the design procedure and the correlations adopted from the literature.

Finally, the design procedure may be improved by a variable speed compressor to cope with the variation of the refrigeration load due to different modes of operation.

## REFERENCES

- [1] Mehendale, S. S., Jacobi, A. M., Shah, R. K., “Fluid flow and heat transfer at micro- and meso-scales with applications to heat exchanger design”, *Applied Mechanics Review*, vol. 53, pp. 175–193, 2000.
- [2] Kandlikar, S. G., Grande, W. J. “Evolution of microchannel flow passages, thermo-hydraulic performance and fabrication technology”, *Heat Transfer Engineering*, 24: 1, 3 – 17, 2003.
- [3] Serizawa, A., Feng, Z., Kawara, Z., “Two-phase flow in microchannels”, *Exp. Therm. Fluid Sci.*, 26(6-7), 703-714, 2002.
- [4] Kew, P. A., Cornwell, K., “Correlations for the prediction of boiling heat transfer in small-diameter channels”, *Applied Thermal Engineering*, 17(8-10), 705-715, 1997.
- [5] Lazarek, G. M., Black, S. H., “Evaporative heat transfer, pressure drop and critical heat flux in a small vertical tube with R-113”, *International Journal of Heat Mass Transfer*, 25, 945–960, 1982.
- [6] Yan, Y. Y., Lin, T. F., “Evaporation heat transfer and pressure drop of refrigerant R-134A in a small pipe”, *International Journal of Heat and Mass Transfer*, 41, 4183–4194, 1998.

- [7] Agostini, B., Bontemps, A., “Vertical flow boiling of refrigerant R-134A in small channels”, *International Journal of Heat and Fluid Flow*, 26, 296-306, 2005.
- [8] Owhaib, W., Palm, B., “Flow boiling heat transfer in a vertical circular microchannel tube”, *Proceedings of Eurotherm Seminar*, No. 72, Valencia, Spain, 2003.
- [9] Owhaib, W., Martin, C. C., Palm, B., “Evaporative heat transfer in vertical circular microchannels”, *Applied Thermal Engineering*, 24, 1241–1253, 2004.
- [10] Mehendale, S. S., Jacobi, A. M., “Evaporative heat transfer in meso-scale heat exchangers”, *ASHRAE Transactions: Symposia*, Dallas, TX, 445–452, 2000.
- [11] Huo, X., Chen, L., Tian, Y. S., Karayiannis, T. G., “Flow boiling and flow regimes in small diameter tubes”, *Applied Thermal Engineering*, 24, 1225–1239, 2004.
- [12] Kandlikar, S. G., Steinke, M. E., “Predicting heat transfer during flow boiling in mini-channels and microchannels”, *ASHRAE Transactions*, 109(1), 1-9, 2003.
- [13] Kandlikar, S. G., Balasubramanian, P., “An extension of the flow boiling correlation to transition, laminar and deep laminar flows in mini-channels and microchannels”, *Heat Transfer Engineering*, 25(3), 86-93, 2004.
- [14] Friedel, L., “New friction pressure drop correlations for upward, horizontal and downward two-phase pipe flow”, *HTFS Symposium*, Oxford, 1979.

- [15] Wilson, M. J., Newell, T. A., Chato, J. C., Infante, F. C. A., "Refrigerant charge, pressure drop and condensation heat transfer in flattened tubes", *Int. J. Refrig.*, 26(4), 442-451, 2003.
- [16] Zhang, M., Webb, R. L., "Correlation of two phase friction for refrigerants in small-diameter tubes", *Exp. Therm. Fluid. Sci.*, 25(3-4), 131-139, 2001.
- [17] Yang, C. Y., Webb, R. L., "Predictive model for condensation in small hydraulic diameter tubes having axial micro fins", *Journal of Heat Transfer*, ASME Transactions, 119(4), 776-782, 1997.
- [18] Koyama, S., Kuwahara, K., Nakashita, K., Yamamoto, K., "An experimental study on condensation of refrigerant R-134A in multi-port extruded tube", *International Journal Refrigeration*, 26(4), 425-432, 2003.
- [19] Shin, J. S., Kim, M. H., "An experimental study of flow condensation heat transfer inside circular and rectangular micro-channels", *Heat Transfer Engineering*, 26(3), 36-44, 2005.
- [20] Chow L.C., Ashraf N.S., Carter III H.C., Casey K., Corban S., Drost M.K., Gumm A.J., Hao Z., Hasan A.Q., Kapat J.S., Kramer L., Newton M., Sundaram K.B., Vaidya J., Wong C.C., Yerkes K., "Design and analysis of a meso-scale refrigerator," *Proceedings of the ASME International Mech. Eng. Congr. and Expos.*, ASME, 1999, pp. 1-8.
- [21] Heydari A., "Miniature vapor compression refrigeration systems for active cooling of high performance computers," *Proceedings of the Inter Society Conference on Thermal Phenomena*, IEEE, 2002, pp. 371-378.
- [22] Phelan P.E., Swanson J., Chiriac F., Chiriac V., "Designing a meso-scale vapor-compression refrigerator for cooling high-power microelectronics,"

Proceedings of the Inter Society Conference on Thermal Phenomena, IEEE, 2004, pp. 218-23.

- [23] Chiriac, F., Chiriac, V., “An alternative method for the cooling of power microelectronics using classical refrigeration”, 2007
- [24] Mongia R., Masahiro K., DiStefano E., Barry J., Weibo C., Izenson M., Possamai F., Zimmermann A., Mochizuki M., "Small scale refrigeration system for electronics cooling within a notebook computer," IEEE, 2006, pp. 751-758.
- [25] Kandlikar, S. G., “Flow boiling in microchannels and mini-channels”, heat transfer and fluid flow in mini-channels and microchannels, 2006
- [26] Kakac, S., Shah, R. K., and Aung, W., Handbook of single phase convective heat transfer, New York: John Willey and Sons, Inc., 1987
- [27] Shah, R. K. and London, A. L., “Laminar flow forced convection in ducts”, Supplement 1 to Advances in Heat Transfer, New York: Academic Press, 1978
- [28] Jaeseon Lee, Issam Mudawar, “Two-phase flow in high-heat-flux micro-channel heat sink for refrigeration cooling applications: Part I—pressure drop characteristics”, Boiling and Two-Phase Flow Laboratory, School of Mechanical Engineering, Purdue University, West Lafayette, IN 47907 1288, USA, 2004
- [29] Kandlikar, S. G., “Single phase liquid flow in microchannels and mini-channels”, Heat Transfer and Fluid Flow in mini-channels and microchannels, 2006

- [30] Gnielinski, V., 1976, "New equations for heat and mass transfer in turbulent pipe and channel flow", *Int. Chem. Engineering*, Vol. 16, pp. 359-368
- [31] Filonenko G.K., "Hydraulic resistance in pipes", *Heat Exchanger Design Handbook*, Teploenergetica Vol 1. No. 4, pp.40-44., 1954
- [32] Celata, G.P., Cuma, M., Zummo, G., "Thermal hydraulic characteristics of single-phase flow in capillary pipes", *Experimental Thermal and Fluid Science*, Vol. 28, Issues 2-3, pp. 87-95, 2004
- [33] Incropera, F.P., DeWitt, D.P., *Fundamentals of heat and mass transfer*, 5<sup>th</sup> Edn., New York: John Wiley and Sons, 2002
- [34] Trabzon, L., "Mikrokanalların üretim metotları", *Mühendis ve Makina Cilt : 47 Sayı: 556, Sayfa 34-50*, 2006
- [35] Acar, Y., "Simulation of vapor compression refrigeration cycle for a household refrigerator", M.S. Thesis, Department of Mechanical Engineering, Middle East Technical University, 1998
- [36] ASHRAE HVAC Fundamentals Handbook, F19, 1997
- [37] Garimella S, "Condensation in mini-channels and microchannels", *Heat Transfer and Fluid Flow in mini-channels and microchannels*, 2006
- [38] Lee, H. J. & Lee, S. Y., "Pressure drop correlations for two-phase flow within horizontal rectangular channels with small heights", *Int. J. Multiphase Flow*, 27(5), 783-796, 2001

- [39] Baroczy, C. J., "Correlation of liquid fraction in two-phase flow with applications to liquid metals", Chem. Eng. Symp. Series, 61(57), 179-191, 1965
- [40] Bandhauer, T. M., "Measurement and modeling of condensation heat transfer coefficients in circular microchannels", Modine Manufacturing Company, Racine, WI 53403, 2006
- [41] Rohsenow, W. M., Hartnett, J. P. and Ganic, E. N., Handbook of heat transfer fundamentals. New York, McGraw-Hill, 1985
- [42] Kim, M.-H. and Bullard, C. W., "Air-side thermal hydraulic performance of multi-louvered fin aluminum heat exchangers," International Journal of Refrigeration, 25 (3): 390-400, 2002
- [43] Chang, Y. J., Wang, C. C., "A generalized heat transfer correlation for louver fin geometry", Int. Journal of Mass Transfer, Vol. 40, No.3, pp533-544, 1997
- [44] Jeong, S., "How difficult is it to make a micro refrigerator?", Int. Journal of Refrigeration, Vol. 27, Issue , pp. 309-313, 2003
- [45] Khan, S. H., "Second-law-based thermodynamic analysis of vapor-compression refrigeration cycles", M.S. Thesis, Department of Mechanical Engineering, King Fahd University of Petroleum and Minerals, Saudi Arabia, 1992

## APPENDIX A

### PRESSURE VS. ENTHALPY CURVE OF R-134A

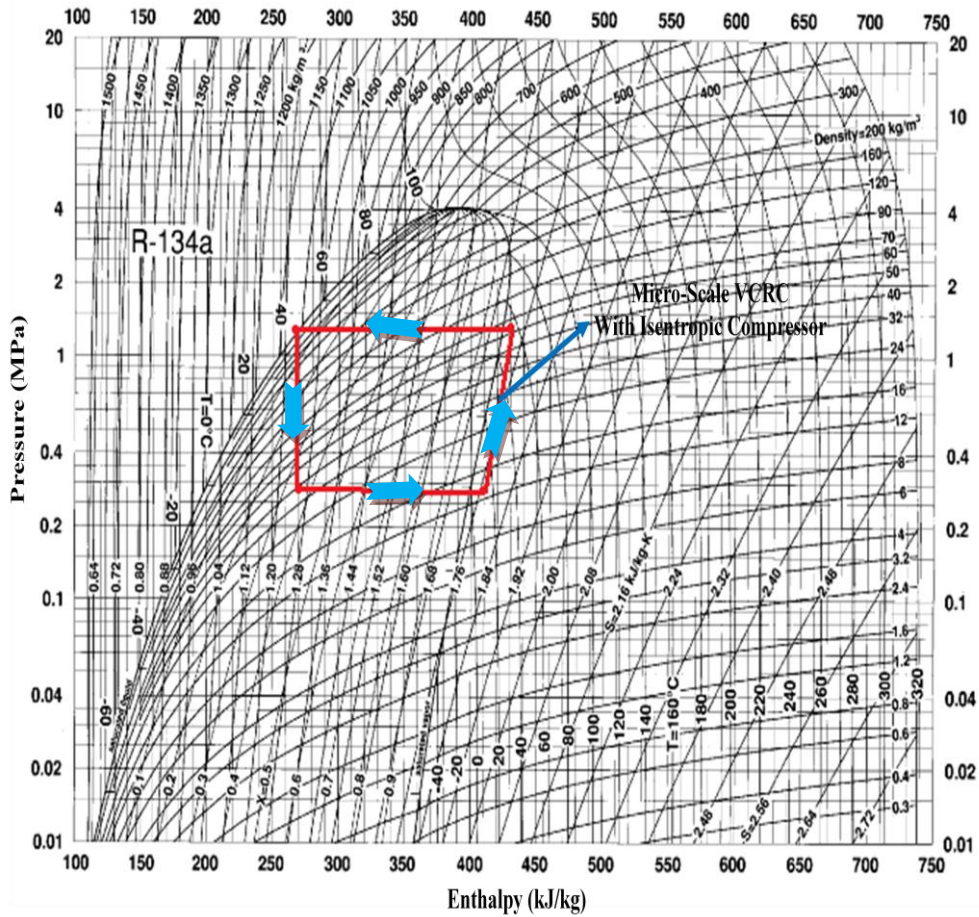


**Figure A. 1** Pressure vs. Enthalpy Curve of R-134A

## APPENDIX B

### SATURATED LIQUID AND VAPOR PROPERTIES OF R-134A

**Table B. 1** Saturation Properties of R-134A

Temp., °C	Absolute Pressure, MPa	Density, kg/m <sup>3</sup>		Enthalpy, kJ/kg		Entropy, kJ/(kg·K)		Specific Heat $c_p$ , kJ/(kg·K)			Velocity of Sound, m/s		Viscosity, μPa·s		Thermal Cond., mW/(m·K)		Surface Tension, mN/m	Temp., °C
		Liquid	Vapor	Liquid	Vapor	Liquid	Vapor	Liquid	Vapor	Liquid	Vapor	Liquid	Vapor	Liquid	Vapor			
-103.0a	0.0039	1591.2	35.263	71.89	335.07	0.4143	1.9638	1.147	0.585	1.163	1135	127	2186.6	6.63	—	—	28.15	-103.30
-100.00	0.0056	1581.9	25.039	75.71	337.00	0.4366	1.9456	1.168	0.592	1.161	1111	128	1958.2	6.76	—	—	27.56	-100.00
-90.00	0.0153	1553.9	9.7191	87.59	342.94	0.5032	1.8975	1.201	0.614	1.155	1051	131	1445.6	7.16	—	—	25.81	-90.00
-80.00	0.0369	1526.2	4.2504	99.65	349.03	0.5674	1.8585	1.211	0.637	1.151	999	134	1109.9	7.57	—	—	24.11	-80.00
-70.00	0.0801	1498.6	2.0528	111.78	355.23	0.6286	1.8269	1.215	0.660	1.148	951	137	879.6	7.97	125.8	—	22.44	-70.00
-60.00	0.1594	1471.0	1.0770	123.96	361.51	0.6871	1.8016	1.220	0.685	1.146	904	139	715.4	8.38	121.1	—	20.81	-60.00
-50.00	0.2948	1443.1	0.60560	136.21	367.83	0.7432	1.7812	1.229	0.712	1.146	858	142	594.3	8.79	116.5	7.12	19.22	-50.00
-40.00	0.5122	1414.8	0.36095	148.57	374.16	0.7973	1.7649	1.243	0.740	1.148	812	144	502.2	9.20	111.9	8.19	17.66	-40.00
-30.00	0.8436	1385.9	0.22596	161.10	380.45	0.8498	1.7519	1.260	0.771	1.152	765	145	430.4	9.62	107.3	9.16	16.13	-30.00
-28.00	0.9268	1380.0	0.20682	163.62	381.70	0.8601	1.7497	1.264	0.778	1.153	756	145	418.0	9.71	106.3	9.35	15.83	-28.00
-26.076	1.0132	1374.3	0.19016	166.07	382.90	0.8701	1.7476	1.268	0.784	1.154	747	146	406.4	9.79	105.4	9.52	15.54	-26.076
-26.00	1.0164	1374.1	0.18961	166.16	382.94	0.8704	1.7476	1.268	0.785	1.154	747	146	406.0	9.79	105.4	9.53	15.53	-26.00
-24.00	1.1127	1368.2	0.17410	168.70	384.19	0.8806	1.7455	1.273	0.791	1.155	738	146	394.6	9.88	104.5	9.71	15.23	-24.00
-22.00	1.2160	1362.2	0.16010	171.26	385.43	0.8908	1.7436	1.277	0.798	1.156	728	146	383.6	9.96	103.6	9.89	14.93	-22.00
-20.00	1.3268	1356.2	0.14744	173.82	386.66	0.9009	1.7417	1.282	0.805	1.157	719	146	373.1	10.05	102.6	10.07	14.63	-20.00
-18.00	1.4454	1350.2	0.13597	176.39	387.89	0.9110	1.7399	1.286	0.812	1.159	710	146	363.0	10.14	101.7	10.24	14.33	-18.00
-16.00	1.5721	1344.1	0.12556	178.97	389.11	0.9211	1.7383	1.291	0.820	1.160	700	147	353.3	10.22	100.8	10.42	14.04	-16.00
-14.00	1.7074	1338.0	0.11610	181.56	390.33	0.9311	1.7367	1.296	0.827	1.162	691	147	344.0	10.31	99.9	10.59	13.74	-14.00
-12.00	1.8516	1331.8	0.10749	184.16	391.55	0.9410	1.7351	1.301	0.835	1.164	682	147	335.0	10.40	99.0	10.76	13.45	-12.00
-10.00	2.0052	1325.6	0.09963	186.78	392.75	0.9509	1.7337	1.306	0.842	1.166	672	147	326.3	10.49	98.0	10.93	13.16	-10.00
-8.00	2.1684	1319.3	0.09246	189.40	393.95	0.9608	1.7323	1.312	0.850	1.168	663	147	318.0	10.58	97.1	11.10	12.87	-8.00
-6.00	2.3418	1313.0	0.08591	192.03	395.15	0.9707	1.7310	1.317	0.858	1.170	654	147	309.9	10.67	96.2	11.28	12.58	-6.00
-4.00	2.5257	1306.6	0.07991	194.68	396.33	0.9805	1.7297	1.323	0.866	1.172	644	147	302.2	10.76	95.3	11.45	12.29	-4.00
-2.00	2.7206	1300.2	0.07440	197.33	397.51	0.9903	1.7285	1.329	0.875	1.175	635	147	294.7	10.85	94.3	11.62	12.00	-2.00
0.00	2.9269	1293.7	0.06935	200.00	398.68	1.0000	1.7274	1.335	0.883	1.178	626	147	287.4	10.94	93.4	11.79	11.71	0.00
2.00	3.1450	1287.1	0.06470	202.68	399.84	1.0097	1.7263	1.341	0.892	1.180	616	147	280.4	11.03	92.5	11.96	11.43	2.00
4.00	3.3755	1280.5	0.06042	205.37	401.00	1.0194	1.7252	1.347	0.901	1.183	607	147	273.6	11.13	91.6	12.13	11.14	4.00
6.00	3.6186	1273.8	0.05648	208.08	402.14	1.0291	1.7242	1.353	0.910	1.187	598	147	267.0	11.22	90.7	12.31	10.86	6.00
8.00	3.8749	1267.0	0.05284	210.80	403.27	1.0387	1.7233	1.360	0.920	1.190	588	147	260.6	11.32	89.7	12.48	10.58	8.00
10.00	4.1449	1260.2	0.04948	213.53	404.40	1.0483	1.7224	1.367	0.930	1.193	579	146	254.3	11.42	88.8	12.66	10.30	10.00
12.00	4.4289	1253.3	0.04636	216.27	405.51	1.0579	1.7215	1.374	0.939	1.197	569	146	248.3	11.52	87.9	12.84	10.02	12.00
14.00	4.7276	1246.3	0.04348	219.03	406.61	1.0674	1.7207	1.381	0.950	1.201	560	146	242.5	11.62	87.0	13.02	9.74	14.00
16.00	5.0413	1239.3	0.04081	221.80	407.70	1.0770	1.7199	1.388	0.960	1.206	550	146	236.8	11.72	86.0	13.20	9.47	16.00
18.00	5.3706	1232.1	0.03833	224.59	408.78	1.0865	1.7191	1.396	0.971	1.210	541	146	231.2	11.82	85.1	13.39	9.19	18.00
20.00	5.7159	1224.9	0.03603	227.40	409.84	1.0960	1.7183	1.404	0.982	1.215	532	145	225.8	11.92	84.2	13.57	8.92	20.00
22.00	6.0777	1217.5	0.03388	230.21	410.89	1.1055	1.7176	1.412	0.994	1.220	522	145	220.5	12.03	83.3	13.76	8.65	22.00
24.00	6.4566	1210.1	0.03189	233.05	411.93	1.1149	1.7169	1.420	1.006	1.226	512	145	215.4	12.14	82.4	13.96	8.38	24.00
26.00	6.8531	1202.6	0.03003	235.90	412.95	1.1244	1.7162	1.429	1.018	1.231	503	144	210.4	12.25	81.4	14.15	8.11	26.00
28.00	7.2676	1194.9	0.02829	238.77	413.95	1.1338	1.7155	1.438	1.031	1.238	493	144	205.5	12.36	80.5	14.35	7.84	28.00
30.00	7.7008	1187.2	0.02667	241.65	414.94	1.1432	1.7149	1.447	1.044	1.244	484	143	200.7	12.48	79.6	14.56	7.57	30.00
32.00	8.1530	1179.3	0.02516	244.55	415.90	1.1527	1.7142	1.457	1.058	1.251	474	143	196.0	12.60	78.7	14.76	7.31	32.00
34.00	8.6250	1171.3	0.02374	247.47	416.85	1.1621	1.7135	1.467	1.073	1.259	465	142	191.4	12.72	77.7	14.97	7.05	34.00
36.00	9.1172	1163.2	0.02241	250.41	417.78	1.1715	1.7129	1.478	1.088	1.267	455	142	186.9	12.84	76.8	15.19	6.78	36.00
38.00	9.6301	1154.9	0.02116	253.37	418.69	1.1809	1.7122	1.489	1.104	1.276	445	141	182.5	12.97	75.9	15.41	6.52	38.00
40.00	1.0165	1146.5	0.01999	256.35	419.58	1.1903	1.7115	1.500	1.120	1.285	436	140	178.2	13.10	75.0	15.64	6.27	40.00
42.00	1.0721	1137.9	0.01890	259.35	420.44	1.1997	1.7108	1.513	1.138	1.295	426	140	174.0	13.24	74.1	15.86	6.01	42.00
44.00	1.1300	1129.2	0.01786	262.38	421.28	1.2091	1.7101	1.525	1.156	1.306	416	139	169.8	13.38	73.1	16.10	5.76	44.00
46.00	1.1901	1120.3	0.01689	265.42	422.09	1.2185	1.7094	1.539	1.175	1.318	407	138	165.7	13.52	72.2	16.34	5.51	46.00
48.00	1.2527	1111.3	0.01598	268.49	422.88	1.2279	1.7088	1.553	1.196	1.331	397	137	161.7	13.67	71.3	16.59	5.26	48.00
50.00	1.3177	1102.0	0.01511	271.59	423.63	1.2373	1.7078	1.569	1.218	1.345	387	137	157.7	13.83	70.4	16.84	5.01	50.00
52.00	1.3852	1092.6	0.01430	274.71	424.35	1.2468	1.7070	1.585	1.241	1.360	377	136	153.8	13.99	69.5	17.10	4.76	52.00
54.00	1.4553	1082.9	0.01353	277.86	425.03	1.2562	1.7061	1.602	1.266	1.377	367	135	149.9	14.16	68.5	17.36	4.52	54.00
56.00	1.5280	1073.0	0.01280	281.04	425.68	1.2657	1.7051	1.621	1.293	1.395	358	134	146.1	14.33	67.6	17.63	4.28	56.00
58.00	1.6033	1062.8	0.01212	284.25	426.29	1.2752	1.7041	1.641	1.322	1.416	348	133	142.3	14.51	66.7	17.91	4.04	58.00
60.00	1.6815	1052.4	0.01146	287.49	426.86	1.2847	1.7031	1.663	1.354	1.438	338	132	138.6	14.71	65.8	18.19	3.81	60.00
62.00	1.7625	1041.7	0.01085	290.77	427.37	1.2943	1.7019	1.686	1.388	1.463	328	131	134.9	14.91	64.9	18.48	3.57	62.00
64.00	1.8464	1030.7	0.01026	294.08	427.84	1.3039	1.7007	1.712	1.426	1.490	318	129	131.2	15.12	63.9	18.78	3.34	64.00
66.00	1.9334	1019.4	0.00970	297.44	428.25	1.3136	1.6993	1.740	1.488	1.522	308	128	127.5	15.35	63.0	19.09	3.12	66.00
68.00	2.0234	1007.7	0.00917	300.84	428.61	1.3234	1.6979	1.772	1.515	1.557	298	127	123.9	15.59	62.1	19.40	2.89	68.00
70.00	2.1165	995.6	0.00867	304.29	428.89	1.3332	1.6963	1.806	1.567	1.597	287	126	120.3	15.85	61.2	19.72	2.67	70.00
72.00	2.2130	983.1	0.00818	307														

## APPENDIX C

### SAMPLE CALCULATIONS

Sample calculations are given for the micro-scale VCRC with the original evaporator and the isentropic compressor.

#### C.1 Evaporator Part

##### C.1.1 Two-Phase Region

- $H = 0.4$  mm
- $w = 0.5$  mm
- $t = 0.5$  mm
- $L_{initial} = 0.129$  m
- $q = 45$  W
- $w_o = N_{ch} (w + t) + t = 0.0105$  m
- $q'' = q / (L w_o) = 3.2967 \times 10^5$  W/m<sup>2</sup>
- $A_{flow} = N H w = 2 \times 10^{-6}$  m<sup>2</sup>
- $P = 2 N (H + w) = 0.0180$  m
- $D_h = 4 \frac{A_{flow}}{P} = 4.4444 \times 10^{-4}$  m
- $G = \frac{\dot{m}}{A_{flow}} = 175$  W/m<sup>2</sup> K
- $Re_l = G D_h \frac{1-x}{\mu_l} = 86.56$

- $Re_v = G D_h \frac{x}{\mu_v} = 4835.6$
- $a_c = 0.8$
- $P_o = 24 (1 - (1.3553 a_c) + (1.9467 a_c^2) - (1.7012 a_c^3) + (0.9564 a_c^4) - 0.2537 a_c^5) = 14.3818$
- $f_l = \frac{P_o}{Re_l} = 0.1662$
- $f_v = (1.82 \log(Re_v) - 1.64)^{-2} = 0.0390$
- $\frac{\Delta P_l}{L} = \frac{2 f_l G^2 (1-x)^2}{D_h \rho_l} = 1810.6 \text{ Pa/m}$
- $\frac{\Delta P_v}{L} = \frac{2 f_v G^2 x^2}{D_h \rho_v} = 1.7230 \times 10^5 \text{ Pa/m}$
- $We_l = G^2 \frac{D_h}{\rho_l \sigma} = 0.8985$
- $X = \sqrt{\frac{(\frac{\Delta P}{L})_l}{(\frac{\Delta P}{L})_v}} = 0.1025$
- $C = 1.45 (Re_l^{0.25}) (We_l^{0.23}) = 4.3152$
- $\phi_l^2 = 1 + \left(\frac{C}{X}\right) + \left(\frac{1}{X^2}\right) = 138.2554$
- $\frac{\Delta P_f}{L} = \frac{\Delta P_l}{L} \phi_l^2 = 2.5033 \times 10^5 \text{ Pa/m}$
- $\Delta P_{acc} = G^2 \vartheta_{lv} (x_2 - x_1) = 1343.4 \text{ Pa}$
- $\Delta P_{tot} = \Delta P_f + \Delta P_{acc} = 4597.7 \text{ Pa}$
- $Nu_{lo} = 3.3461$
- $Bo = \frac{q''}{G i_{lv}} = 0.0095$
- $Co = \left(\frac{1-x}{x}\right)^{0.8} \sqrt{\frac{\rho_v}{\rho_l}} = 0.0577$
- $h_{tp} = 0.6883 Co^{-0.2} (1-x)^{0.8} h_{lo} + (1058 Bo^{0.7} (1-x)^{0.8} S h_{lo}) = 19030 \text{ W/m}^2\text{K}$
- $\tau_{fin} = \frac{\tanh(m_{fin} L_c)}{m_{fin} L_c} = 0.99$
- $L_c = H = 0.4 \times 10^{-3} \text{ m}$
- $m_{fin} = \left(2 \frac{h}{k_{Cu} t_{ch}}\right)^{0.5} = 435.684$

- $T_b = T_{CR} - \left( q'' \frac{t_{base}}{k_{copper}} \right) = 14.1779 \text{ } ^\circ\text{C}$
- $\Delta T = T_b - T = 14.1779 \text{ } ^\circ\text{C}$
- $L = \frac{q}{h_{tp} (2 H \tau_{fin} + t_{ch}) N \Delta T} = 12.9 \times 10^{-3} \text{ m}$

### C.1.2 Single-Phase Region

- $L_{initial} = 0.054 \text{ m}$
- $\Delta T = 3 \text{ } ^\circ\text{C}$
- $Re = G \frac{D_h}{\mu_{sp}} = 6840.6$
- $Nu_{GN} = \left( \frac{f}{8} \right) (Re - 1000) \frac{Pr_{sp}}{1 + 12.7 \sqrt{\frac{f}{8}} \left( Pr_{sp}^{\frac{2}{3}} - 1 \right)} = 23.6515$
- $f = (1.82 \log(Re) - 1.64)^{-2} = 0.0351$
- $Nu = Nu_{GN} (1 + F) = 34.155$
- $F = C Re \left( 1 - \left( \frac{D_h}{D_o} \right)^2 \right) = 0.4441$
- $D_o = 1.164 \times 10^{-3} \text{ m}$
- $C = 7.6 \times 10^{-5}$
- $h = Nu \frac{k_{sp}}{D_h} = 966 \text{ W/m}^2\text{K}$
- $\Delta P = f \left( \frac{1}{2} \right) \rho_{sp} U m_{sp}^2 \left( \frac{L}{D_h} \right) = 480.87 \text{ Pa}$
- $m_{fin} = \left( 2 \frac{h}{k_{Cu} t_{ch}} \right)^{0.5} = 98.1621$
- $\tau_{fin} = \frac{\tanh(m_{fin} L_c)}{m_{fin} L_c} = 0.9995$
- $L = \frac{q}{h_{sp} (2 H \tau_{fin} + t_{ch}) N \Delta T} = 5.4 \times 10^{-3} \text{ m}$

## C.2 Compressor Part

- $N = 500$  rpm
- $V_p = \frac{\dot{m} v_1}{\eta_{vol} N} \times 60 = 4.3635 \times 10^{-6} \text{m}^3$
- $V_p = \pi \frac{D^2}{4} L_{st} = 4.3635 \times 10^{-6} \text{m}^3$
- $L/D = 5$
- $D = 10.4$  mm
- $L = 51.8$  mm
- $V_c = C V_p = 2.1818 \times 10^{-7} \text{m}^3$
- $P_s = P_1 f_{ps} = 2.7323 \times 10^5 \text{Pa}$
- $P_d = \frac{P_2}{f_{pd}} = 1.3873 \times 10^6 \text{Pa}$
- $k \cong \frac{c_p}{c_v} = 1.1360$
- $W = \dot{m} (i_1 - i_4) = 11.0915 \text{W}$
- $\eta_{cl.} = 1 + C - C \left( \frac{P_d}{P_s} \right)^{\frac{1}{k}} = 0.8502$
- $\eta_{vol.} = (1 + C) \left( \frac{P_s}{P_1} \right)^{\frac{1}{k}} - C * \left( \frac{P_d}{P_1} \right)^{\frac{1}{k}} - f_{leakage} \left( \frac{P_d}{P_s} \right) = 0.7531$
- $N_{comp.} = \frac{\dot{m} v_1}{\eta_{vol} V_p} \times 60 = 500$  rpm
- $U_{mpiston} = 2 L \frac{N_{comp.}}{60} = 0.8631$  m/s.

## C.3 Condenser Part

- $A_{flow} = N \pi \frac{D^2}{4} = 1.9635 \times 10^{-6} \text{m}^2$
- $P = N \pi D = 0.0157$  m
- $D_h = 4 \frac{A_{flow}}{P} = 0.5 \times 10^{-3} \text{m}$
- $A_{free_a} = (L_{seg} - N_{fin} z_t) z_l = 1.6214 \times 10^{-4} \text{m}$

- $P_a = 4 \left( L_{seg} - N_{fin} z_t + \frac{z_l}{2} \right) = 0.0892 \text{ m}$
- $D_{ha} = 4 \frac{A_{freea}}{P_a} = 0.0073 \text{ m}$

### C.3.1 Single-Phase Region

- $T_1 = 58.05 \text{ }^\circ\text{C}$
- $T_2 = 50 \text{ }^\circ\text{C}$
- $T_{ai} = 30 \text{ }^\circ\text{C}$
- $L = 14 \text{ mm}$
- $Re = G \frac{D_h}{\mu_{sp}} = 6294.3$
- $Nu_{GN} = \left( \frac{f}{8} \right) (Re - 1000) \frac{Pr_{sp}}{1 + 12.7 \sqrt{\frac{f}{8}} \left( Pr_{sp}^{\frac{2}{3}} - 1 \right)} = 24.1232$
- $f = (1.82 \log(Re) - 1.64)^{-2} = 0.036$
- $F = C Re \left( 1 - \left( \frac{D_h}{D_o} \right)^2 \right) = 0.3901$
- $Nu = Nu_{GN} (1 + F) = 33.5341$
- $h = Nu \frac{k_{sp}}{D_h} = 1164.3 \text{ W/m}^2\text{K}$
- $\Delta P = f \left( \frac{1}{2} \right) \rho_{sp} U m_{sp}^2 \left( \frac{L}{D_h} \right) = 249.32 \text{ Pa}$
- $f_a = (Re_{lp}^{-0.781}) \left( \frac{\theta}{90} \right)^{0.444} \left( \frac{z_p}{l_p} \right)^{-1.682} \left( \frac{z_l}{l_p} \right)^{-1.22} \left( \frac{z_d}{l_p} \right)^{0.818} \left( \frac{l_l}{l_p} \right)^{1.97} = 0.2351$
- $Re_{lp} = G_a \frac{l_p}{\mu_a} = 247.83$
- $j_{colb} = 1.18 (Re_{lp}^{-0.505}) \left( \frac{\theta}{90} \right)^{0.26} \left( \frac{z_l}{l_p} \right)^{-0.51} \left( \frac{z_d}{l_p} \right)^{-0.26} \left( \frac{l_l}{l_p} \right)^{0.82} \left( \frac{t_p}{l_p} \right)^{-0.25} \left( \frac{z_t}{l_p} \right)^{-0.097} = 0.029$
- $h_a = j_{colb} C p_a \rho_a U m_a Pr_a^{-\frac{2}{3}} = 182.86 \text{ W/m}^2\text{K}$
- $\Delta P_a = f_a G_a^2 \frac{z_d}{2 \rho_a l_p} = 44.5 \text{ Pa}$

- $Power = \Delta P_a \frac{\dot{m}_a}{\rho_a} = 0.0221 \text{ W}$
- $U_o = \frac{1}{\left(\frac{A_o}{A_i h_i}\right) + \left(\frac{1}{h_a \tau_{fin_o}}\right)} = 42.5309 \text{ W/m}^2\text{K}$
- $\tau_{fin_a} = \frac{\tanh(m_{fin} Lc_{fin})}{m_{fin} Lc_{fin}} = 0.7563$
- $\tau_{fin_o} = 1 - \left(\frac{A_{fin}}{A_{tot}}\right) (1 - \tau_{fin_a}) = 0.7795$
- $m_{fin} = \left(2 \frac{h_a}{k_{fin} z_t}\right)^{0.5} = 110.2303$
- $Lc_{fin} = (fin_l) + \left(\frac{fin_t}{2}\right) = 0.0092$
- $NTU = U_o \frac{A_o}{C_{min}} = 0.4054$
- $C_{min} = \dot{m}_t C_p = 0.4431 \text{ W/K}$
- $q_{max} = q_{max} C_{min} (T_{hi} - T_{ci}) = 12.429 \text{ W}$
- $C_r = \frac{C_{min}}{C_{max}} = 0.7769$
- $\epsilon = 1 - \exp\left(\frac{-NTU}{C_r}\right) \left(\exp(-C_r * NTU) - 1\right) = 0.2858$
- $q = q_{max} \epsilon = 3.5526 \text{ W}$

### C.3.2 Two-Phase Region

Calculations are given for the first segment:

- $x_1 = 1$
- $x_2 = 0.6467$
- $L = 50 \times 10^{-3} \text{ m}$
- $T_{ai} = 30 \text{ }^\circ\text{C}$
- $f_i = A X^a Re_l^b \varphi^c f_l = 0.0355$
- $\varphi = j_l \frac{\mu_l}{\sigma} = 0.0136$
- $j_l = G \frac{1-x}{\rho_l (1-\alpha_v)} = 0.4306 \text{ m/s}$

- $A = 1.308 \times 10^{-3}$     $a = 0.427$     $b = 0.930$
- $c = -0.121$     $f_l = \frac{64}{Re} = 1.3106$
- $Re_l = G D_h \frac{1-x}{\mu_l (1+\sqrt{a_v})} = 48.83$
- $Re_v = G D_h \frac{x}{\mu_v \sqrt{a_v}} = 5528.3$
- $a_v = \left(1 + \left(\frac{1-x}{x}\right)^{0.74} \left(\frac{\rho_v}{\rho_l}\right)^{0.65} \left(\frac{\mu_l}{\mu_v}\right)^{0.13}\right)^{-1} = 0.9361$
- $X = \left(\frac{1-x}{x}\right)^{0.9} \left(\frac{\rho_v}{\rho_l}\right)^{0.5} \left(\frac{\mu_l}{\mu_v}\right)^{0.1} = 0.075$
- $\Delta P = \left(\frac{1}{2}\right) f_i G^2 \frac{x^2}{\rho_v a_v^{2.5}} \frac{L}{D_h} = 692.5 \text{ Pa}$
- $h = \rho_l c p_l \frac{u^*}{T^+} = 3880.3 \text{ W/m}^2\text{K}$
- $u^* = \sqrt{\frac{\tau_i}{\rho_l}} = 0.039$
- $\tau_i = \left(\frac{\Delta P}{L}\right) \sqrt{a_v} \frac{D_h}{4} = 1.6751 \text{ Pa}$
- $T^+ = 5 Pr_l + 5 \ln \left( Pr_l \left(\frac{\delta^+}{5} - 1\right) + 1 \right) = 17.37$
- $\delta^+ = \delta \rho_l \frac{u^*}{\mu_l} = 2.2107$
- $\delta = (1 - \sqrt{a_v}) \frac{D_h}{2} = 8.1141 \times 10^{-6} \text{ m}$
- $\Delta P_{bend_{two-phase}} = \Delta P_{bend_{liq}} \left(1 + \frac{2x\rho_{liq}}{\rho_r}\right) = 716.815 \text{ Pa}$
- $\Delta P_{bend} = \left(\frac{1}{2}\right) k_{minor} \rho_r V_r^2 = 83.83 \text{ Pa}$
- $f_a = (Re_{lp}^{-0.781}) \left(\frac{\theta}{90}\right)^{0.444} \left(\frac{z_p}{l_p}\right)^{-1.682} \left(\frac{z_l}{l_p}\right)^{-1.22} \left(\frac{z_d}{l_p}\right)^{0.818} \left(\frac{l_l}{l_p}\right)^{1.97} = 0.2351$
- $Re_{lp} = G_a \frac{l_p}{\mu_a} = 247.83$
- $Um_a = \frac{G_a}{\rho_a} = 4.376 \text{ m/s}$
- $\Delta P_a = f_a G_a^2 \frac{z_d}{2 \rho_a l_p} = 44.5 \text{ Pa}$

$$\begin{aligned}
- j_{colb} &= 1.18 (Re_{lp}^{-0.505}) \left(\frac{\theta}{90}\right)^{0.26} \left(\frac{z_l}{l_p}\right)^{-0.51} \left(\frac{z_d}{l_p}\right)^{-0.26} \left(\frac{l_l}{l_p}\right)^{0.82} \\
&\quad \left(\frac{t_p}{l_p}\right)^{-0.25} \left(\frac{z_t}{l_p}\right)^{-0.097} = 0.029 \\
- h_a &= j_{colb} C p_a \rho_a U m_a Pr_a^{-\frac{2}{3}} = 182.86 \text{ W/m}^2\text{K} \\
- Power &= \Delta P_a \frac{\dot{m}_a}{\rho_a} = 0.0789 \text{ W} \\
- \tau_{fin_o} &= 1 - \left(\frac{A_{fin}}{A_{tot}}\right) (1 - \tau_{fin_a}) = 0.7795 \\
- \tau_{fin_a} &= \frac{\tanh(m_{fin} L c_{fin})}{m_{fin} L c_{fin}} = 0.7563 \\
- m_{fin} &= \left(2 \frac{h_a}{k_{fin} * fin_t}\right)^{0.5} = 110.2303 \\
- L c_{fin} &= (fin_l) + \left(\frac{fin_t}{2}\right) = 0.0092 \text{ m} \\
- U_o &= \frac{1}{\left(\frac{A_o}{A_i h_i}\right) + \left(\frac{1}{h_a \tau_{fin_o}}\right)} = 83.5755 \text{ W/m}^2\text{K} \\
- C_{min} &= m_a C_{p,a} = 2.0369 \text{ W/K} \\
- q_{max} &= C_{min} (T_{ri} - T_{ai}) = 40.7370 \text{ W} \\
- NTU &= U_o \frac{A_o}{C_{min}} = 0.6190 \\
- \epsilon &= 1 - \exp(-NTU) = 0.4615 \\
- q_{tot} &= q_{max} \epsilon = 18.8007 \text{ W} \\
- T_{ao} &= T_{ai} + (q_{tot}/(\dot{m}_a C p_a)) = 37 \text{ }^\circ\text{C}
\end{aligned}$$

For the rest of the segments, the results of calculations are given in Table C.1 and C.2.

**Table C. 1** Refrigerant Side Results

Refrigerant Side	Segment 2	Segment 3	Segment 4
$x_{in}$	0.6467	0.3236	0.702
$x_{out}$	0.3236	0.0702	0
L (mm)	50	50	20
G (kg/m <sup>2</sup> s)	178.25	178.25	178.25
$\dot{m}$ (g/s)	0.35	0.35	0.35
Q (W)	17.2	13.5	3.78
$\Delta P$ (Pa)	581.7	316.5	62.5
Re <sub>l</sub>	153.6	256.5	356.5
Re <sub>v</sub>	3457	1582	426.9
V <sub>l</sub> (m/s)	0.0836	0.1307	0.1561
V <sub>v</sub> (m/s)	1.3019	0.5166	0.0945
h (W/m <sup>2</sup> K)	2959	1684	911.1

**Table C. 2 Air Side Results**

Air Side	Segment 2	Segment 3	Segment 4
L (mm)	50	50	20
G (kg/m <sup>2</sup> s)	5	5	5
$\dot{m}$ (g/s)	2	2	0.81
V <sub>a</sub> (m/s)	4.376	4.376	4.376
Re <sub>lp</sub>	247.83	247.83	247.83
j <sub>colb</sub>	0.029	0.029	0.029
f	0.2351	0.2351	0.2351
ΔP (Pa)	44.5	44.5	44.5
T <sub>ao</sub> (°C)	38.44	36.6	34.6
ε	0.4221	0.331	0.2317
η <sub>o</sub>	0.7795	0.7795	0.7795
h <sub>a</sub> (W/m <sup>2</sup> K)	182.86	182.86	182.86
U <sub>o</sub> (W/m <sup>2</sup> K)	74.03	54.3	33.6

**C.4 Capillary Tube Part**

Calculations are given for the first segment of the capillary tube.

- $T_1 = 50\text{ }^\circ\text{C}$
- $T_1 = 40\text{ }^\circ\text{C}$
- $x_1 = 0$
- $x_2 = 0.0934$
- $Re = \frac{4 \dot{m}}{\pi D \mu} = 7380.5$
- $V_1 = \frac{\vartheta_1 \dot{m}}{A_c} = 2.5274\text{ m/s}$

- $V_2 = \frac{\vartheta_2 \dot{m}}{A_c} = 7.4897 \text{ m/s}$
- $f = 0.33 Re^{-0.25} = 0.0356$
- $\Delta L_1 = \frac{-\Delta P - G \Delta V}{\left(\frac{G}{2D}\right) (f V)_{mean}} = 0.4629 \text{ m}$

For the rest segments, the results are given in Table A.4.

**Table C. 3** Capillary Tube Results

Segment:	2	3	4	5
T <sub>1</sub> (°C)	40	30	20	10
T <sub>2</sub> (°C)	30	20	10	0
x <sub>1</sub>	0.0934	0.1728	0.2422	0.3042
x <sub>2</sub>	0.1728	0.2422	0.3042	0.3603
Re	7133.7	6895.3	6659.4	6420.8
V <sub>1</sub> (m/s)	7.4026	14.7765	26.03	43.46
V <sub>2</sub> (m/s)	14.8459	26.0869	43.5	71.015
f	0.0359	0.0362	0.0365	0.0369
ΔL (m)	0.1623	0.0648	0.0245	0.0061